HAL
open science

Vasculogenic mimicry, a complex and devious process favoring tumorigenesis -Interest in making it a therapeutic target

Lucas Treps, Sébastien Faure, Nicolas Clere

To cite this version:

Lucas Treps, Sébastien Faure, Nicolas Clere. Vasculogenic mimicry, a complex and devious process favoring tumorigenesis -Interest in making it a therapeutic target. Pharmacology & Therapeutics Part A Chemotherapy Toxicology and Metabolic Inhibitors, 2021, 223, pp.107805. 10.1016/j.pharmthera.2021.107805 . inserm-03349934

HAL Id: inserm-03349934

https://inserm.hal.science/inserm-03349934

Submitted on 21 Sep 2021

HAL is a multi-disciplinary open access archive for the deposit and dissemination of scientific research documents, whether they are published or not. The documents may come from teaching and research institutions in France or abroad, or from public or private research centers.

L'archive ouverte pluridisciplinaire **HAL**, est destinée au dépôt et à la diffusion de documents scientifiques de niveau recherche, publiés ou non, émanant des établissements d'enseignement et de recherche français ou étrangers, des laboratoires publics ou privés.

Vasculogenic mimicry, a complex and devious process favoring tumorigenesis – Interest in making it a therapeutic target

Lucas Treps[(1)], Sébastien Faure[(2)], Nicolas Clere[(2)]

(1) Université de Nantes, CNRS, INSERM, CRCINA, F-44000 Nantes, France

(2) Micro et Nanomédecines Translationnelles, MINT, UNIV Angers, UMR INSERM 1066, UMR CNRS 6021, Angers, France

Correspondence :

Nicolas Clere – Pharm D., Ph D

Inserm UMR 1066 CNRS 6021

IBS – CHU Angers

4, rue Larrey

F-49933 Angers Cedex

nicolas.clere@univ-angers.fr

Abstract

Tumor cell vasculogenic mimicry (VM), also dubbed vascular mimicry, describes the plasticity of aggressive cancer cells forming *de novo* vascular networks and is associated with the malignant phenotype and poor clinical outcome. VM is described in a plethora of tumors, including carcinomas, sarcomas, glioblastomas, astrocytomas and melanomas. The presence of VM is associated with a high tumor grade, short survival, invasion and metastasis. A variety of molecular mechanisms and signal pathways participates in VM induction and formation. Due to VM's contribution on tumor progression, more VM-related strategies are being utilized for anticancer treatment. After describing the main features of VM, this review will outline the importance of the tumor microenvironment during this process, and highlight the predominant molecular targets and signaling pathways involved. These data will make it possible to discuss the importance of VM-associated mediators in antitumor therapy and how it could allow to better understand the resistance to anticancer therapy.

Keywords: Cancer cells; tumor microenvironment; vessels; signaling pathways; endothelial cells; anticancer therapy

56 **Table of Contents**

57 **1. Introduction**

58 **2. Characteristics of vascular mimicry**

59 *2.1. Epithelial-mesenchymal transition and VM*

60 2.2. *Tumor microenvironment, team spirit in VM*

61 **3. Molecular mechanisms in VM**

62 *3.1. VEGF signaling beyond angiogenesis, involvement in VM*

63 *3.2. CSC-related VEGF signaling in VM*

64 *3.3. VE-cadherin, more than an endothelial marker*

65 *3.4. VE-PTP, a VE-cadherin-associated receptor*

66 *3.5. EphA2 signaling in VM*

67 *3.6. MMPs, powerful modelers of the tumor microenvironment*

68 *3.7. Semaphorins, potential guides in VM*

69 *3.8. Notch signaling in VM*

70 *3.9. COXs inflammation in VM*

71 *3.10. Non-coding RNAs*

72 **4. VM and cancer therapy**

73 *4.1. Cancer resistance*

74 *4.2. Therapeutic targeting of VM*

75 **5. Conclusion**

76

77

78

Abbreviations

αSMA: alpha smooth muscle actin
CAF: cancer-associated fibroblast
COX2: cyclo-oxygenase 2
CSC: cancer stem cell
Dll: Delta-like ligand
EMT: epithelial-mesenchymal transition
EphA2: ephrin A2 receptor
EVs: extracellular vesicles
FAK: focal adhesion kinase
GSC: glioblastoma stem-like cell
HCC: hepatocellular carcinoma
HDAC: histone deacetylase
HIF: hypoxia-inducible factor
lncRNA: long non-coding RNA
LOXL2: lysyl oxidases like 2
miRNA: micro-RNA
MMP: matrix metalloproteinase
ncRNA: non-coding RNA
NSCLC: non-small cell lung cancer
PAS: periodic acid-Schiff
PGE2: prostaglandin E2
PI3K: phosphatidylinositol-3-kinase
TAM: tumor-associated macrophage
TGF-ß: transforming growth factor beta
TME: tumor microenvironment
uORF: upstream open reading frame
VEGF: vascular endothelial growth factor
VE-PTP: vascular endothelial protein tyrosine phosphatase
VM: vasculogenic mimicry

110 **1. Introduction**

111 Since the studies of Judah Folkman (Folkman, 1971) supplemented by those of Napoleone
112 Ferrara (Kim et al., 1993), tumor growth and metastasis have been explained by a change in
113 the tumor vascular structure through angiogenesis and vasculogenesis. Formation of the
114 tumor vasculature was largely thought to parallel physiological processes of
115 neovascularization, with endothelial sprouting and proliferation being the principal routes of
116 new blood vessel formation. However, this dogma was discussed after the demonstration by
117 Maniotis *et al*. in 1999 (Maniotis et al., 1999) of vascular mimicry (VM) in malignant
118 melanoma. In these tumors, the patterned vascular channels characteristic of aggressive
119 primary and metastatic melanoma are different from angiogenic vessels in that vascular
120 channels in aggressive melanomas are embedded in highly patterned matrix whereas
121 angiogenic vessels are characterized by clusters of vessels and are not patterned.
122 Furthermore, the patterned melanoma vascular channels were not found to be lined by
123 endothelium whereas the contribution of an endothelium to angiogenic vessels is clearly
124 identified. The hypothesis proposed to explain this new vascular architecture was a process
125 of dedifferentiation of tumor cells into an endothelial-like phenotype whose clinical
126 implications are clear: VM-forming tumors were more aggressive than their non-VM
127 counterparts (Qin et al., 2019). Furthermore, VM-lined channels might not respond
128 predictably to conventional anti-angiogenic therapies in melanoma (Schnegg et al., 2015) or
129 other cancers (Angara et al., 2017; Hori et al., 2019).

130 A major controversial commentary has been proposed on the topic entitled
131 "Vasculogenic mimicry: how convincing, how novel and how significant" (McDonald et al.,
132 2000). Briefly, the main criticisms raised from this commentary focused on different aspects
133 of the original and rather descriptive VM study, which led the authors to the following

134 questions: (i) Can the VM structures be considered as blood vessels and do they contribute
135 meaningfully to blood flow? (ii) Can the presence or absence of endothelial cells and tumor
136 cells surrounding the vascular lumen be established using unambiguous markers? (iii) Is there
137 an interface between endothelial cells and tumor cells in blood vessel walls? Thus, the
138 relevance of the conclusions from Maniotis *et al*. was questioned, considering the possibility
139 that perhaps VM channels were not functional (Maniotis et al., 1999). Moreover, there were
140 serious technical limitations in identifying VM channels using conventional
141 immunohistochemistry which was prone to artifacts and not entirely objective. Despite these
142 criticisms, it seems that VM has re-entered the spotlight in cancer research with several
143 publications in journal with good scientific impact (Williamson et al., 2016; Xiang et al., 2018)
144 and also with a significant publication rate in the last 10 years (940 hits on *Pubmed* with
145 keywords "vascular mimicry cancer" or "vasculogenic mimicry cancer"). These last studies
146 provide the basis to better define tumor VM which is the source of many resistance to
147 anticancer therapies and also explain the aggressiveness of certain tumors.
148

149 **2. Characteristics of vascular mimicry**

150 During its vascular stage, tumor nutrition through diffusion is no longer sufficient and
151 expansion of new vasculature is necessary for tumor growth (Folkman, 1990; Gimbrone et al.,
152 1972). Presently, five vascularization modes are now recognized (Carmeliet and Jain, 2011):
153 sprouting and intussusceptive angiogenesis, vessel co-option (Kuczynski et al., 2019),
154 endothelial cell transdifferentiation and VM.

155 VM is defined as the formation of new blood vessels following the acquisition of
156 vascular cell features or functions by tumor cells of a non-vascular origin. Two distinct VM
157 types have been identified: tubular and patterned matrix VM. Patterned VM is composed of

158 an extracellular matrix of irregular thickness, that is positive for periodic acid-Schiff (PAS),
159 laminin or heparan sulfate, and surrounding islets of cancer cells (Fig. 1A). Although patterned
160 VM networks are shown to conduct fluids, the patterned matrix does not contain a continuous
161 lumen and is morphologically different than blood vessels or their vascular matrix (Folberg
162 and Maniotis, 2004; Maniotis et al., 1999). Furthermore, tubular VM is composed of tumor
163 cells that mimic the normal endothelium to form hollowed and perfused tube-like channels
164 (El Hallani et al., 2010) (Fig. 1B). Whilst blood and lymph vessels are formed by a monolayer
165 of endothelial cells surrounded by a semi-continuous basement membrane, tubules from VM
166 are formed by cancer cells resting on an inner glycoprotein rich matrix (Fig. 2) (Valdivia et al.,
167 2019). In this review, unless specified, the term VM encompasses both tubular and patterned
168 VM types.

169 Ongoing discussions in the field suggest a minimal set of experiments which needs to
170 be performed in order to ascertain the occurrence of VM. Historically, both *in vivo* and *in vitro*
171 models VM structures were positively stained with PAS, and they did not possess endothelial
172 markers such as CD31 or CD34 (Maniotis et al., 1999). Although immunohistology and
173 molecular studies have highlighted the expression of endothelial markers (CD31, CD34, VE-
174 cadherin) in VM structures, $PAS^{+}/CD31^{-}$ staining is currently the most widely used marker for
175 VM. *In vitro*, the molecular characteristics underlying VM are traditionally confirmed in models
176 of highly invasive cell lines able to form tubes on Matrigel®. Finally, the functionality of hollow
177 VM structures has been confirmed *in vitro* upon dye perfusion, and in tumor biopsies with the
178 presence of red blood cells in VM structure's lumen (Ruf et al., 2003; Sood et al., 2001). To
179 date, the occurrence of VM has been shown in various pre-clinical models of breast
180 (Wagenblast et al., 2015), ovarian, prostate (Liu et al., 2012), astrocytoma, glioblastoma,
181 hepatocellular carcinoma (HCC) and lung cancers. Depending on the cancer type, the

182 incidence of VM positive tumors (based on PAS+CD31- staining) varies considerably (5 to 65%)
183 (Valdivia et al., 2019). However, these investigations need to be taken with a pinch of salt and
184 backed-up by rigorous tissue examination (McDonald et al., 2000).
185

186 *2.1. Epithelial-mesenchymal transition and VM*

187 VM formation is a sophisticated process involving various mechanisms. While similarities have
188 been shown between epithelial-mesenchymal transition (EMT) and VM, several studies have
189 stressed the main role of tumor microenvironment (TME) during VM.

190 Initially, EMT has been recognized as a key step during embryonic morphogenesis
191 (Nieto et al., 2016). In different pathophysiological conditions, including cancer, EMT involves
192 various cellular changes in which epithelial cells loosen (i) their attachments to neighboring
193 cells and (ii) their apico-basal cell polarity, while (iii) they start acquiring mesenchymal markers
194 including vimentin, N-cadherin and fibronectin (Thiery, 2002). EMT is highly dynamic, implying
195 transient (dubbed partial-EMT) and reversible states (Ribatti et al., 2020), as well as direct cell-
196 cell interaction or secreted cues (reviewed in (Kim et al., 2020)). EMT implies different
197 signaling pathways including (among other) TGF-β, Wnt, Notch and Hedgehog (Chen et al.,
198 2016; Islam et al., 2016; Ma et al., 2018), as well as the expression of specific transcription
199 factors (Snail, Twist1, SOX4 and ZEB1) acting as repressors of epithelial markers (Gil et al.,
200 2016; Leskela et al., 2019; Ma et al., 2018). This transcriptional remodeling is accompanied by
201 a cadherin switching (Wheelock et al., 2008), particularly from E-cadherin to a panel of
202 mesenchymal cadherins (N-, P-, R-, T- and cadherin 11), that was correlated with tumor
203 progression and invasiveness in squamous cell carcinomas (Miro et al., 2019) and endometrial
204 adenocarcinoma (Fan et al., 2019). Thus, during EMT, cancer cells trade their epithelial
205 characteristics to mesenchymal traits including cytoskeleton reorganization and higher

206 motility (Sannino et al., 2017). Altogether, initiating the first step of the invasion–metastasis
207 cascade, detrimental for patient's prognosis and raising cancer death-toll (Pastushenko and
208 Blanpain, 2019).

209 Interestingly, several studies have shown that EMT is involved in VM formation (Fig. 2,
210 inset i). As proof, it has been reported that ZEB1 small hairpin RNA inhibits both the formation
211 of VM and EMT in triple negative breast cancer (Liang et al., 2018) and colorectal cancer
212 models (Liu et al., 2012). Likewise, it has been found that Twist1 is able to regulate VM
213 formation in astrocytoma, and that its expression is associated with the grade of astrocytoma,
214 one of the most vascularized types tumor in human (Cao et al., 2019; Li et al., 2020). Thus, it
215 suggests a non-negligible role of VM in glioma tumor vascularization. In HCC cell lines,
216 chromatin immunoprecipitation and luciferase assays demonstrated that Twist1 binds the VE-
217 cadherin promoter region and induces VE-cadherin transcription (a molecule which function
218 is developed further below) (Sun et al., 2010). In breast cancer cell lines, Twist1 could mediate
219 VM formation by transcriptional repression of claudin 15 (Zhang et al., 2020). Moreover, in
220 HCC model, it has been confirmed that Twist1 regulates VM formation abilities, through the
221 VE-cadherin/AKT pathway (Sun et al., 2010). Wnt signaling is involved in various physiological
222 processes, such as tumor cell proliferation (Yang et al., 2017), endothelial cell differentiation,
223 and angiogenesis (Shetti et al., 2019). Furthermore, several studies suggested that Wnt
224 signaling induces EMT by repressing glycogen synthase kinase-3β (GSK3β)-mediated
225 phosphorylation that subsequently regulates the phosphorylation/degradation of Snail, an
226 important mediator of EMT (reviewed elsewhere in (Zhong et al., 2020)). Initially, it has been
227 reported that Wnt/β-catenin signaling was involved in VM formation in colon cancer (Qi et al.,
228 2015). Recently, the mechanistic basis of osteosarcoma VM has been extended to 143B and

229 HOS cell lines where microarray analyzes showed enriched TGF-β and Wnt signaling pathway
230 (Yao et al., 2020).
231 TGF-β is one of the key EMT driver in various pathologies including cancer (Wendt et al.,
232 2009). Thus, it is not unfounded to assume that TGF-β signaling pathway may also regulate
233 VM. As such, *in vitro* and clinical studies observed that (i) HCC patients with VM and ZEB2
234 nuclear expression have a shorter survival period than those without expression, and (ii) ZEB2
235 promotes VM by TGF-β induced EMT (Yang et al., 2015b). Moreover, in a model of SHG44
236 glioma cells transfected with TGF-β cDNA, EMT regulated by p38/MAPK signaling pathways
237 could participate in VM formation, suggesting a role of this cytokine in the unfavorable
238 evolution of glioma (Ling et al., 2016). As an integral part of the EMT, TGF-β drives the cadherin
239 switching with a loss of E-cadherin and an increase of N-cadherin. Seemingly, VEGF-A plays a
240 similar role during the hypoxia-induced VM in salivary adenoid cystic carcinoma (Wang et al.,
241 2019) and various models of liver tumor (Chen et al., 2019). Thus, these findings suggest that
242 the signaling pathways involved in EMT and VM formation are likely identical or perhaps
243 complementary. A thorough transcriptomic meta-analysis of several VM-competent and TGF-
244 β-treated cancer cell lines could help clarifying this point.
245
246 2.2. *Tumor microenvironment, team spirit in VM*
247 The tumor microenvironment (TME) is the sophisticated cellular milieu in which the tumor
248 develops. Apart from the tumor cells, TME comprises blood and lymphatic vessels, the
249 extracellular matrix and other non-malignant cells including cancer stem cells (CSCs),
250 fibroblasts or immune cells (Wu et al., 2017). Several factors deeply influence the TME and
251 are thus powerful modulators of cell's behaviors. In the following sections, we discuss new
252 findings about how cells from TME contribute to the process of VM (Fig. 2).

253 *Cancer stemness properties and VM*

254 CSCs are rare subpopulations of neoplastic cells within a tumor, usually less than 5%, which
255 are able to generate new tumors in appropriate animal hosts. CSCs have been first identified
256 in human acute myeloid leukemia in 1994, where authors showed that cancer cells grafted
257 into SCID mice produce a large number of $CD34^{+}/CD38^{-}$ subpopulation of leukemic cells
258 (Lapidot et al., 1994). CSCs are also expressed in several solid tumor entities such as breast
259 (Yue et al., 2018), brain (Ren et al., 2018), colon (Lenos et al., 2018), gastric (Zavros, 2017) or
260 prostate (Gorodetska et al., 2019) cancers. Additionally, evidence point out that these CSCs
261 are the cause of tumor initiation, progression, invasion, metastasis, chemoradiotherapy
262 resistance, and relapse underscoring their paramount importance in tumorigenesis (Peitzsch
263 et al., 2017). Among the hypotheses behind the formation of VM, this process would be the
264 ability of VM tumor cells to adopt the pluripotent phenotype of embryonic cells (Seftor et al.,
265 2002). CSC marker expressions associated with VM in human malignant tumors suggest that
266 CSCs may participate in the formation of VM (Fig. 2, inset ii). Different biomarkers are used to
267 characterize and identify CSCs. CD133, also called prominin-1, is a common biomarker of CSCs
268 that was initially described as a biomarker in human hematopoietic stem and progenitor cells
269 (Yin et al., 1997). Currently, CD133 overexpression in various human cancers is considered a
270 significant (unifying?) marker of CSCs (Aghajani et al., 2020; Lathia et al., 2015; Wang et al.,
271 2020b). $CD133^{+}$ tumor cells are able to induce tumor cell proliferation (Pavon et al., 2018),
272 metastasis (Liou, 2019) and to differentiate into other kinds of cells (Virant-Klun et al., 2019;
273 Zhang et al., 2020). Aldehyde dehydrogenase 1 (ALDH1) is another biomarker of CSCs in liver,
274 lung, ovarian, gastric, colorectal or breast cancer (Tomita et al., 2016), and described as a
275 potent inducer of tumor cell proliferation, differentiation and oxidative stress (Vishnubalaji et
276 al., 2018; Zhou et al., 2020). Different studies conducted on various tumor types have shown

277 a correlation between an increase of CD133 and ALDH1 expression, and VM formation. For
278 instance, in osteosarcoma, an aggressive malignant bone tumor in children and adolescents,
279 positive rates of CD133, ALDH1 and VM are significantly higher in tumor tissues compared
280 with control tissues, and positively associated with lymph node and distant metastasis, as well
281 as poor patient overall survival (Bao et al., 2018). In HCC, CD133 and VM are also reported to
282 be significantly higher in tumor tissues than in normal liver tissues (Xu et al., 2018a). Recently,
283 in human and mice triple-negative breast cancer models, it has been confirmed that $CD133^+$
284 and $ALDH1^+$ cells form more VM channels *in vivo* (Sun et al., 2019). These results confirmed
285 CSCs as crucial modulators in the process of VM formation.

286 Because human neural stem cells have been shown to transdifferentiate into
287 endothelial cells (Wurmser et al., 2004), it is established that the differentiation of CSCs into
288 endothelial cells represents one of the hypotheses explaining VM formation. Indeed, renal
289 CSCs can generate endothelial cells *in vitro* and give rise to vessels with a human origin *in vivo*
290 (Bussolati et al., 2008). Furthermore, human breast CSCs undergo endothelial differentiation
291 to generate functional endothelial cells *in vitro* and *in vivo* (Bussolati et al., 2009).
292 Subsequently, these data, obtained from *in vitro* studies, were supplemented by more robust
293 pre-clinical and clinical studies. Thus, in glioblastoma, it has been reported that CSCs generate
294 endothelial cells that form $CD105^+$ (endoglin) tumor vessels (Wang et al., 2010). Moreover,
295 Ricci-Vitiani *et al*. showed that a broad range (20-90%) endothelial cells in glioblastoma
296 harbors the same chromosomal alterations as in tumor cells (Ricci-Vitiani et al., 2010).
297 Although controversial, these studies demonstrate that CSCs in multiple tumors have
298 endothelial differentiation abilities and could contribute to VM formation. This fact is
299 supported by a study conducted on human glioblastoma samples, showing that the so-called
300 glioblastoma stem-like cells (GSCs) may differentiate into $CD31^+/CD34^+$ endothelial cells and

301 promote VM formation (Mei et al., 2017). In another study conducted on HCC1937/p53 cells,
302 derived from triple-negative breast cancer, cancer cell-transdifferentiated endothelial cells
303 expressed endothelial markers such as VE-cadherin, matrix metalloproteinase (MMP)-2 and -
304 9 and exhibited VM formation ability on Matrigel® (Izawa et al., 2018). Besides, in a mouse
305 embryonic stem cell-induced model of lung CSCs, these cells were able to transdifferentiate
306 into an endothelial cell-like phenotype expressing CD31 and capable of forming tubes on 3D
307 matrix (Prieto-Vila et al., 2016). Taken together, cancer cell's plasticity and transdifferentiation
308 clearly contribute to VM formation. However, presently the exact mechanism driving
309 transdifferentiation and a common underlying signaling across cancer types are lacking but
310 may be worth investigating for therapeutic purpose (see further below).
311
312 *Hypoxia and VM*
313 Intratumoral hypoxia, which is commonly observed in various solid tumors (Denko, 2008),
314 could trigger numerous signaling pathways which may lead to adverse clinical outcomes
315 including higher cancer invasiveness through promotion of tumor metastasis, EMT or
316 angiogenesis (Chiu et al., 2019) (Fig. 2). Among different hypoxia-related pathways, hypoxia-
317 inducible factors (HIFs) have been studied extensively (Wigerup et al., 2016). As major
318 transcriptional regulators in response to hypoxia, HIFs consist of an oxygen-regulated HIF-α
319 subunit (HIF-1α or HIF-2α) dimerizing with HIF-1β under hypoxia. The dimer then complexes
320 with CREB-cAMP-response element binding protein and activates the transcription of a
321 panoply of target genes harboring hypoxia responsive elements (HRE). Various studies have
322 evaluated the influence of oxygen decrease in the regulation of EMT and VM formation. For
323 instance, Du *et al*. confirmed that hypoxia contributes to VM formation by inducing EMT.
324 Interestingly, HIF-1α expression, analyzed by immunohistochemistry in 71 specimens of

325 epithelial ovarian cancers, was correlated with loss of E-cadherin expression and up-regulated
326 vimentin expression in 61% of VM-positive patients. Moreover, ovarian cancers with evidence
327 of VM were significantly more likely to have high Twist1, Slug and VE-cadherin expression
328 levels under hypoxia. *In vitro*, ovarian cancer cells presented morphological EMT-like changes
329 under hypoxic conditions (Du et al., 2014). Furthermore, an association of HIF-1α expression
330 and VM formation has been reported in other solid cancers such as melanoma or HCC. An
331 interesting study has confirmed that HIF-1α promotes VM formation in HCC through lysyl
332 oxidases like 2 (LOXL2, a secreted copper-dependent amine oxidase) up-regulation in hypoxic
333 TME. Thus, from clinical HCC tissues, HIF-1α, LOXL2 expression and CD31/PAS double staining
334 were examined by immunohistochemical staining and correlated to poor prognosis. These
335 data have been backed up by series of *in vitro* assays that confirmed a positive relationship
336 between hypoxia, HIF-1α and LOXL2 protein. Thus, HIF-1α was found to induce EMT, HCC cell
337 migration, invasion and VM formation by regulating LOXL2 (Wang et al., 2017). Hence, hypoxia
338 appears as a critical player during EMT and VM formation, and could act on several intricate
339 pathways.
340
341 *Cancer-associated fibroblasts and VM*
342 Cancer-associated fibroblasts (CAFs) are major components of stromal cells that surround
343 cancer cells, and control proliferation, survival, angiogenesis, metastasis, immunogenicity and
344 resistance to therapies (Su et al., 2018). CAFs constitute the main pool of collagen-producing
345 cells, which directly communicate with cancer cells and various cells from the TME such as
346 endothelial or inflammatory cells. However, the biological properties of CAFs are disparate
347 with different types of CAF driving distinct functional contributions. Besides, previous studies
348 indicated that CAFs arise from different sources of origin including local infiltrating fibroblast,

349 epithelial or endothelial cells, pericytes or adventitial fibroblasts of the vascular system, or
350 cancer cells themselves undergoing fibroblastic transformation, which may explain CAF's
351 morphological, phenotypical and functional variability (Chen and Song, 2019). In this context,
352 it has been proposed that CAFs could be determinant in VM formation (Fig. 2, inset iii). Thus,
353 in a recent study, VM-competent murine melanoma cells endogenously expressing the
354 matricellular protein CCN2 (also named CTGF), were injected in mice carrying a CAF-specific
355 CCN2 deletion. Interestingly, the absence of fibroblast-derived CCN2 reduced tumor
356 vasculature, including VM occurrence (Hutchenreuther et al., 2018). Furthermore, PAS^+
357 tissues from human cutaneous melanoma were also positive for the vascular pericyte marker
358 α-smooth muscle actin (αSMA) within the extracellular matrix networks lined by tumor cells.
359 Moreover, when VM-competent tumor cells were co-cultured with pericytes, there was a
360 striking stabilization of the VM networks for up to 96 h (Thijssen et al., 2018). We could parallel
361 these findings with the fact that in glioblastoma, VM structures co-express αSMA and PDGFR,
362 another vascular pericyte marker (Francescone et al., 2012; Scully et al., 2012). The
363 importance of CAFs has also been found in gastric cancers where they promote tumorigenesis
364 through EphA2 (Hong et al., 2018; Nakamura et al., 2005). Pioneer studies in melanoma have
365 previously correlated the activation of the EphA2 receptor tyrosine kinase with VM formation
366 (Hess et al., 2001; Hess et al., 2006) (developed further below). Consequently, EphA2 was
367 significantly associated with VM formation in head and neck squamous cell carcinoma (Wang
368 et al., 2014) and gastric cancer cells (Kim et al., 2019b), which process was lowered in both
369 cases upon EphA2 knockdown. These findings were supplemented by a recent study in gastric
370 cancer AGS cells, showing that VM tube formation was significantly induced by CAF-derived
371 secretome, while conditioned media from normal fibroblasts derived from the same patient
372 had no effect. EphA2 silencing strategy in gastric cancer cells revealed that the CAF-mediated

373 VM promoting effect was mediated through the EphA2-PI3K pathway (Kim et al., 2019a).
374 Altogether, these data suggest that CAFs, as powerful modeler of the TME, may have an
375 underappreciated (yet) function in promoting VM formation.
376
377 *Tumor-associated macrophages and VM*
378 Both innate and adaptive immune cells are present and interact with the tumor cells *via* direct
379 contact or through chemokine and cytokine signaling which shape the behavior of the tumor
380 and its response to therapy. It is well established that tumor-associated macrophages (TAMs)
381 are key regulators in the TME. In solid tumors, the main source of TAM is circulating
382 monocytes rather than proliferating resident macrophages inside tumors. Macrophages can
383 be categorized into M1 and M2 subtypes based on their polarization status. M1 macrophages
384 can be activated by Th1 cytokine interferon gamma and microbial products, while M2
385 macrophages differentiate in response to Th2 cytokines such as IL-4, IL-10 or IL-13 (Qian and
386 Pollard, 2010). In this context of TAMs, M1 macrophages are considered to exert tumoricidal
387 properties whereas M2 macrophages promote tumorigenesis. Both M1 and M2 TAM
388 phenotypes are plastic and reversible, and the TME plays a major role in the regulation of their
389 functional polarization (Duluc et al., 2009; Hagemann et al., 2008). Since inflammatory
390 microenvironment is involved in angiogenesis and plasticity of tumor cells, it has been
391 assumed that inflammatory microenvironment might also promote VM formation (Fig. 2, inset
392 iv). Thus, the infiltration of macrophages in VM-positive areas and the role and underlying
393 mechanism of M2 macrophages in inducing VM formation have been studied in glioblastoma
394 cells (Rong et al., 2016; Zhang et al., 2017). As such, the capability of channel formation in U87
395 cells with or without coculture with M2 (IL-4 stimulated) macrophages has been evaluated.
396 The results revealed that M2 macrophages could enhance the ability to generate vascular

397 channels in U87 cells under normal oxygen condition. The high αSMA and barely detectable
398 VE-cadherin expression in U87 cells proved that these vascular channels consisted of mural-
399 like cells transdifferentiated from tumor cells. To gain additional insights into the mechanism
400 by which M2 macrophages promote VM formation in U87 cells, the proinflammatory cyclo-
401 oxygenase 2 (COX-2) signaling was investigated in the coculture model. Interestingly, COX-2
402 expression and the secretion of its downstream effector prostaglandin E2 (PGE2) were up-
403 regulated in U87 cells after M2 macrophages coculture. Hence suggesting that M2
404 macrophages could induce VM via up-regulating COX-2 expression in glioblastoma cells (Rong
405 et al., 2016). Seemingly, M2-like macrophages enhanced VM through amplification of IL-6
406 secretion by cancer cells (Zhang et al., 2017). These studies highlight intercellular
407 communications (between M2-like macrophages and glioma cells) that induce VM formation
408 *via* the involvement of different pro-inflammatory mediators.

409 Within the TME, several factors can influence the outcome and progression of
410 tumorigenesis. For instance, hypoxia and inflammation contribute to cancer cell plasticity,
411 which could reinforce both EMT and VM (Fig. 2). Concomitantly, tumor-associated
412 macrophages are also important mediators of TME by altering tumor inflammatory status,
413 and interacting with several stromal cells. Finally, growing evidences suggest that CAFs and
414 mural cells are likely to contribute and stabilize VM network formation. In depth *in vivo*
415 profiling would be required to properly assess cellular interactions occurring during VM. In
416 particular, we envision that state-of-the-art single cell technologies and ligand-receptor
417 prediction algorithms would allow a thorough understanding of VM, but such studies are
418 currently lacking.

419

420 **3. Molecular mechanisms in VM**

421 In the following section, we discuss latest insights into the molecular mechanism and signaling
422 pathways driving VM. Non-coding RNA molecules, acting as important epigenetics modifiers,
423 will also be discussed in the context of VM. While a detailed molecular characterization driving
424 VM is still lacking, this section primarily aims at presenting the most acknowledged
425 mechanisms contributing to VM.
426
427 *3.1. VEGF signaling beyond angiogenesis, involvement in VM*
428 VEGF molecules and its receptors (VEGFRs) are key mediators in physiological (e.g.
429 development and wound healing) and pathological angiogenesis including cancer. VEGF-A, the
430 most studied VEGF member, regulates angiogenesis and vascular permeability by activating
431 VEGFR-1 (FLT-1) and VEGFR-2 (KDR/FLK1), while VEGF-C/-D mostly regulate
432 lymphangiogenesis *via* their receptor VEGFR-3 (FLT-4). In melanoma, the autocrine secretion
433 of VEGF-A is shown to activate PI3K/PKCα and integrin-signaling pathways downstream
434 VEGFR-1, thereby leading to VM (Vartanian et al., 2011). Endothelin 1, through its receptor
435 endothelin-receptor type B (EDNRB), was identified as a melanoma progression marker and is
436 thus associated to an aggressive phenotype (Bittner et al., 2000), and also appeared to play
437 an important role in VM. Indeed, the endothelin 1/EDNRB axis could enhance the expression
438 of VEGFR-3 and its ligands VEGF-C/-D *via* a cross talk involving the activation of c-SRC in a β-
439 arrestin-1-dependent fashion (a pathway also linked to VE-cadherin signaling; see below) (Fig.
440 3A). This cooperative interaction between EDNRB- and VEGFR-3-mediated signaling resulted
441 in the induction of melanoma cell migration and VM tube formation, and was further inhibited
442 upon the concomitant blockade of these two receptors (Spinella et al., 2013). Peroxiredoxin-
443 2 belongs to an important family of antioxidant proteins. In colorectal cancer, peroxiredoxin-
444 2 expression was associated with VM formation and its knockdown reduced VEGFR-2

445 activation, allegedly due to an excessive level of oxidative molecules (Zhang et al., 2015a).
446 Similarly, in Epstein-Barr virus-associated malignancies such as nasopharyngeal and gastric
447 cancers where VM was reported, Epstein-Barr virus infection was shown to induce VEGF
448 expression (Xiang et al., 2018; Xu et al., 2018b). However, the exact contribution of VEGF
449 during nasopharyngeal cancer VM is still a matter of debate. Indeed, a first descriptive study
450 indicated that transient silencing of VEGF-A or VEGFR-1 disrupted tubular structures from
451 nasopharyngeal cancer cells, whereas inhibition of VEGFR-2 did not affect the process. Despite
452 the fact LMP-1 and VEGFR-1 expressions were correlated to VM formation, in-depth
453 investigation of the signaling involved was not further investigated by the authors (Xu et al.,
454 2018b). Moreover, further study in the same Epstein-Barr virus-associated cancer outlined a
455 VEGF-independent mechanism (demonstrated by the means of anti-VEGF blocking antibodies
456 and specific anti-VEGFR inhibitors), which activates the PI3K/AKT/mTOR/HIF-1α signaling
457 cascade to induce VM (Xiang et al., 2018).
458
459 *3.2. CSC-related VEGF signaling in VM*
460 As previously discussed in this review, CSCs are discrete but critical sub-populations
461 influencing tumorigenesis and therapy response. In line with their chemoresistance capacities,
462 CSCs express stemness markers and high levels of drug efflux ATP-binding cassette (ABC)
463 transporters. In melanoma, ABCB5-expressing CSCs co-express Tie-1 and VE-cadherin that are
464 characteristic VM markers in aggressive uveal melanoma cells (Hendrix et al., 2001; Schatton
465 et al., 2008). As compared to $ABCB5^-$ cells, $ABCB5^+$ melanoma cells overexpress VEGFR-1 and
466 preferentially associate with VM structures. As such, VEGFR-1 signaling was important for
467 laminin deposition as VEGFR-1 knockdown xenograft showed reduced VM occurrence and
468 lower tumor growth (Frank et al., 2011). However, melanoma are heterogeneous with some

469 tumors that may initially respond to anti-VEGF therapy while other are intrinsically resistant.
470 Mirroring this clinical observation, VEGF-A inhibition in anti-VEGF responsive xenografts leads
471 to an increase in VM, CSC markers, as well as the induction of the HIF-1α expression (Schnegg
472 et al., 2015), reported to regulate VM and CSC phenotype in other cancers such as HCC (Ma
473 et al., 2011), Ewing sarcoma (van der Schaft et al., 2005), melanoma (Zhang et al., 2009) and
474 breast cancer (Mao et al., 2020). Examining whether HIF-1α inhibition could prevent the
475 increase in VM induction and CSC maintenance following VEGF-A inhibition in melanoma will
476 be an interesting strategy. Further stressing the importance of cellular context and treatment
477 response heterogeneity, Notch 3 knockdown in melanoma cells exhibiting high endogenous
478 levels of this marker led to retarded tumorigenicity *in vivo* through depleting CSC fraction,
479 corroborated with a reduction in VM. In contrast, Notch 3 silencing affected neither tumor
480 growth nor CSCs in a melanoma cell line with relatively low endogenous Notch 3 expression
481 (Hsu et al., 2017). In several cancers the zinc-finger transcription factor Slug is reported to be
482 an essential mediator of Twist1-induced EMT and metastasis. As such, in HCC Slug is critical to
483 maintain CSC subpopulation, VE-cadherin and mesenchymal markers expression, which
484 further contribute to VM formation (Sun et al., 2013).

485 CSCs have been particularly well documented in brain tumors, where VM was reported
486 and correlated to higher aggressiveness and shorter overall survival (El Hallani et al., 2010; Liu
487 et al., 2011a; Liu et al., 2011b; Wang et al., 2013; Wang et al., 2012; Yue and Chen, 2005).
488 Immunohistochemistry analysis showed that VM in glioblastoma is principally composed of
489 mural cells co-expressing VEGFR-2, αSMA and PDGFR – the latter two representing vascular
490 pericyte markers – whilst the endothelial marker CD31 was mostly absent (Francescone et al.,
491 2012; Scully et al., 2012). Patient-derived glioblastoma CSCs, the so-called GSCs, were not
492 capable to form any capillary-like structures *in vitro*. Conversely, this ability was retained by

493 GSC-derived differentiated cells expressing high levels of VEGFR-2 and αSMA, *via* a process
494 dependent on VEGFR-2 and ERK signaling but not of its ligand VEGF (Francescone et al., 2012;
495 Scully et al., 2012). Noteworthy, conflicting reports from another group indicate that VEGF,
496 instead, could stimulate GSC-derived VM, albeit they also describe VEGFR-2 as paramount in
497 inducing VM tube formation (Wu et al., 2017; Yao et al., 2013). These discrepancies could be
498 attributed to the distinct GSC models used: fresh patient-derived *versus* U87 cell line-derived
499 GSCs. Orthotopic mouse tumors with VEGFR-2-silenced GSCs showed decreased tumor
500 growth and $\alpha SMA^{+}CD31^{-}$ vessels without affecting the percentage of mouse $CD31^{+}$ vessels
501 (Scully et al., 2012). Thus, the authors hypothesized that a small population of GSC (<1,5%)
502 could undergo EC transdifferenciation, which participates in tumor angiogenesis as previously
503 described (Ricci-Vitiani et al., 2010; Wang et al., 2010).
504

505 *3.3. VE-cadherin, more than an endothelial marker*

506 VE-cadherin (also known as CD144 or cadherin-5) is a trans-membrane protein crucial for
507 vascular development, as demonstrated by early lethal phenotype in knockout mouse model
508 (Carmeliet et al., 1999). Endothelial VE-cadherin is a key player controlling cell-cell adhesion
509 and barrier properties (see review in (Treps et al., 2013)). *Via* its extracellular calcium domains,
510 VE-cadherin forms cis- or trans-homodimers to support cell-cell adhesion. Besides, the
511 extracellular calcium domain can bind the endothelial transmembrane receptor-type
512 phosphatase VE-PTP (vascular endothelial protein tyrosine phosphatase) to poise endothelial
513 barrier and keep endothelial permeability at low level (Orsenigo et al., 2012). Of note, VE-
514 cadherin's intracellular domain is the target of numerous post-translational modifications
515 including phosphorylation which orchestrate different signaling cascades depending on the
516 cell type considered (see below).

517 Although VE-cadherin is an archetypal marker of endothelial cells, a fundamental study
518 reported its expression in highly aggressive human melanoma cells whilst being absent in
519 poorly aggressive melanoma cells derived from the same patient (Hendrix et al., 2001). Highly
520 metastatic melanoma cells had the ability to form vessel-like network in 3D matrix *in vitro*, but
521 this was hampered upon VE-cadherin silencing or CRISPR-Cas9 knockout (Delgado-Bellido et
522 al., 2019; Hendrix et al., 2001). In aggressive melanoma, the molecular pathways downstream
523 VE-cadherin involve its phosphorylation on Y658 residue (pY658) by the focal adhesion kinase
524 (FAK) (Delgado-Bellido et al., 2019) (Fig. 3B). Indeed, FAK silencing or pharmacological
525 inhibition reduced pY658-VE-cadherin levels, even upon VEGF treatment, and decreased VM
526 tube formation. Interestingly, a nuclear pool of pY658-VE-cadherin in complex with p120 was
527 identified in the metastatic uveal cell line MUM2B (Delgado-Bellido et al., 2019). While this
528 phenomenon was already described for p120 and other cadherins such as E-cadherin, this is
529 a premiere for VE-cadherin and would require further validation in other cancer cell types
530 prone to VM. FAK appears to be paramount in controlling the nuclear pY658-VE-cadherin
531 relocalization, which can then associate in complex with Kaiso, a known transcriptional
532 repressor. Upon interaction and binding with p120, Kaiso-transcription repression' activity is
533 counteracted and the target genes induced. Thus, pY658-VE-cadherin could repress the
534 binding of Kaiso to their target genes, induce the expression of CCND1 and Wnt 11, and thus
535 poise the cells to induce VM *in vitro* (Fig. 3B). This recent report highlights how cancer cells
536 such as melanoma cells could highjack existing pathways to induce VM. Recently, a study has
537 developed an original model of culture by coating plates with a fusion protein consisting of
538 the human VE-cadherin extracellular domain coupled to the immunoglobulin G Fc region (Fig.
539 3B). Strikingly, when the Bel7402 HCC cells were cultured on this substrate, they
540 spontaneously adopted tube-like structures, reminiscent of VM. Concomitant with this

541 cytoskeleton rearrangement, the cells showed an increased expression in VE-cadherin, EphA2,
542 MMP-2/-9 secretion and PAS staining. Phenotypically, these HCC cells demonstrated an
543 increased migration and invasion, and higher levels of pFAK and pY658-VE-cadherin,
544 associated to several EMT markers (Shuai et al., 2020). Altogether, this would indicate that
545 VE-cadherin has a pivotal place in inducing the EMT, PI3K/MMPs and EphA2/FAK/p-VE-
546 cadherin signaling, and thus trigger VM formation (Fig. 3B).
547
548 *3.4. VE-PTP, a VE-cadherin-associated receptor*
549 As mentioned above, the transmembrane receptor-type phosphatase VE-PTP associates with
550 VE-cadherin to prevents its pY658 and thus maintains endothelial permeability at minimal
551 level (Orsenigo et al., 2012). Similarly to VE-cadherin, VE-PTP is found expressed in aggressive
552 melanoma cell lines, albeit absent in non-aggressive forms. Despite the fact that VE-PTP
553 knockdown in HUVECs led to an expected increase in pY658-VE-cadherin (due to the absence
554 of VE-PTP phosphatase activity), in aggressive melanoma cells it provoked a distinct outcome
555 with a sharp reduction in pY658- and VE-cadherin total levels. Interestingly enough,
556 immunoprecipitation experiments pointed out that, in this model, VE-PTP does not interact
557 with VE-cadherin but rather with p120 catenin, which is important to prevent VE-cadherin
558 degradation and to sustain the VE-cadherin nuclear pool (Fig. 3B). Noteworthy, the molecular
559 interactions are different in HUVECs where VE-PTP appears linked to VE-cadherin rather than
560 p120 (Delgado-Bellido et al., 2020). Altogether, this highlight that, albeit mimicking normal
561 endothelial cell function, VE-cadherin and VE-PTP behave differently in aggressive melanoma
562 cells to support VM.
563
564 *3.5. EphA2 signaling in VM*

565 The Ephrin family of receptor tyrosine kinases (Eph) and their membrane-tethered ligands
566 (ephrins) constitutes the vastest family of tyrosine kinase receptor. The Ephrin/Eph signaling
567 is involved in various biological processes throughout development, adulthood and
568 pathogenesis (Kania and Klein, 2016). For instance, EphA2, formerly called ECK (epithelial cell
569 kinase), and its ligand ephrin-A1 have been shown to contribute to pathological tumor
570 angiogenesis, albeit *via* an uncharacterized mechanism. Compared to poorly aggressive
571 melanoma cell lines, EphA2 is overexpressed in most advanced melanoma cell lines (up to 14.8
572 fold-change) (Easty et al., 1995; Hess et al., 2007; Hess et al., 2001) and metastatic melanoma
573 biopsies. Furthermore, it is associated with cancer progression and invasion (Easty et al., 1995;
574 Hess et al., 2007). In metastatic aggressive melanoma cell lines, VE-cadherin expression is
575 instrumental in regulating EphA2 localization at cell-cell adhesion complexes, and EphA2
576 tyrosine phosphorylation. Immunostaining and immunoprecipitation indicate that these two
577 transmembrane proteins form a complex *in vitro*, but this might be indirect and could involve
578 additional signaling molecules (Hess et al., 2006). However, even though VE-cadherin-EphA2
579 co-localization has been demonstrated *in situ* in human melanoma sections, a thorough
580 validation is currently lacking (e.g. tube formation). In gastric adenocarcinoma, a positive
581 association between EphA2 expression and VM is highlighted, and further validation studies
582 in gastric cancer cell line indicate that EphA2 knockdown led to a reduction in 3D tube
583 formation *in vitro* (Kim et al., 2019b). Opposingly, EphA2 overexpression in pancreatic
584 adenocarcinoma (Duxbury et al., 2004) and F10-M3 melanoma cells (Parri et al., 2009)
585 increases cell invasiveness in 3D assays, which is in line with the invasive features of VM cells.
586 The F10-M3 metastatic clone of the widely used B16 mouse melanoma cell line has been
587 shown to not express EphA2 and ephrin-A1. However, ectopic expression of EphA2 leads to
588 its tyrosine auto-phosphorylation and downstream signal transduction *via* FAK activation,

589 suggesting a ligand-independent activation (Parri et al., 2009) (Fig. 3B). We can note here that,
590 as mentioned above in melanoma cells, FAK controls pY658-VE-cadherin and its nuclear
591 localization as well as 3D tube formation (Delgado-Bellido et al., 2019). Therefore, although
592 these studies were not performed using the same melanoma cell line, they indicate a possible
593 link between VE-cadherin, EphA2 and FAK signaling in VM.

594 As with many other receptor tyrosine kinases, EphA2 auto-phosphorylation promotes
595 its endocytic internalization, the first step of exosomal sorting (Tkach and Thery, 2016; Walker-
596 Daniels et al., 2002). Such an autocatalytic EphA2 system needs to be poised by the opposing
597 activity of protein tyrosine phosphatases (PTP) and particularly PTP1B located near the
598 pericentriolar recycling endosomes (Nievergall et al., 2010). Another non classical EphA2
599 signaling mechanism was brought to light by studying the secretion profile of doxorubicin-
600 induced senescent cells, and particularly their extracellular vesicle (EV) content. Upon ROS-
601 induced PTP1B inhibition, EphA2 was shed among small EVs and promoted the ERK-
602 dependent proliferation of recipient breast cancer cells through a EphA2/ephrin-A1 reverse
603 signaling (Takasugi et al., 2017). Notwithstanding EphA2 phosphorylation has been linked to
604 VM (Hess et al., 2001; Hess et al., 2006), to our knowledge no study has yet considered the EV
605 communication during VM tube formation (although several studies carried out conditioned
606 media treatments). Additionally, other EphA2 post-translational modifications such as
607 ubiquitination, which balances the EphA2 membranous *versus* internalization remains
608 uncharacterized regarding VM (Sabet et al., 2015).

609

610 *3.6. MMPs, powerful modelers of the tumor microenvironment*

611 These endopeptidases of the zinc-dependent family are implicated in a large variety of
612 physiological processes including wound healing and organogenesis, as well as in pathological

613 conditions including tumorigenesis. All 28 MMPs are produced as proenzymes, and require a
614 post-translational proteolytic cleavage to generate mature MMPs that have proteolytic
615 activity against a broad range of substrates located on the extracellular matrix. As an example,
616 the substrates from MMP-2/-9 include aggrecan, collagens, elastin, fibronectin, laminins, and
617 glycosaminoglycans. MT1-MMP is a membrane-type collagenase which activates the MMP-
618 2/TIMP-2 complex (Fig. 3A), and is considered as a key mediator of cancer progression, EMT
619 and metastasis (Kessenbrock et al., 2010). Additionally, MMPs play a crucial role in reshaping
620 cell-cell and cell-matrix adhesive characteristics, as well as the extracellular matrix, all
621 processes occurring during VM. As such, first evidence came from the group of Mary J.C.
622 Hendrix with microarray analyses revealing that the expression of several MMPs, MT1-MMP,
623 TIMP-1 and laminin-γ2 were fostered in highly *versus* poorly aggressive patient-derived
624 cutaneous melanoma cell lines (Seftor et al., 2001). Beside, MMP-1/-2/-9, MT1-MMP and
625 laminin-γ2 immunostaining showed a preferential expression in 3D tubular structures formed
626 by aggressive ovarian and melanoma cell lines (Sood et al., 2001) and confirm that MT1-MMP
627 is required for VM tube formation (Fig. 3A).

628 The Rictor/mTORC2 complex can phosphorylate AKT at Ser473, thereby activating a
629 central component in the PI3K-AKT pathway that regulates the expression of several MMPs.
630 In melanoma cells, Rictor silencing decreased VM channels formation, cell migration and
631 invasion, pSer473-AKT and the expression of MMP-2/-9 (Liang et al., 2017). Myoferlin, a type
632 II membrane protein, is also a regulator of MMP-2 expression and vouch for adequate VM
633 (tube formation and expression of EMT markers) in A375 human cutaneous melanoma cell
634 line (Zhang et al., 2018). Likewise, supporting initial findings in melanoma and ovarian cancers,
635 a recent study in large cell lung cancer cell lines indicates that recombinant MMP-2 could
636 enhance tube formation ability, while recombinant MMP-13 (collagenase-3) or its ectopic

637 overexpression in H460 and H661 cell lines decreased VM formation (Li et al., 2017a). In
638 melanoma and large cell lung cancer cell lines, the same group showed that while MMP-2
639 proteolytically cleaves laminin-5 into the 105 kD laminin-5γ2' and 80 kD laminin-5γ2x, MMP-
640 13 can generate small laminin-5 fragments (20 to 40 kD). MMP-13-digested laminin-5 could
641 decrease 3D tube formation but enhanced melanoma cell invasion in Transwell assay (Li et al.,
642 2017a; Zhao et al., 2015). The authors hypothesized that MMP-13 proteolytic action may lead
643 to the cleavage of the laminin-5γ2-containing EGF domain, thereby curbing EGFR downstream
644 Raf/ERK/AKT signaling, as well as the rearrangement of F-actin, vimentin and α-tubulin (Li et
645 al., 2017a). Overall, high MMP-13 expression was inversely correlated with VM occurrence in
646 melanoma patients and H460 subcutaneous tumors, and associated to metastasis in patients
647 (Li et al., 2017a; Zhao et al., 2015). MMP-13 expression was also correlated to poorer overall
648 survival of melanoma patients but this could be attributed to endothelium-dependent tumor
649 vascularization rather than VM (Zigrino et al., 2009).

650 Fine-tuning histone acetylation pattern by means of histone deacetylases (HDACs) is
651 an important process controlling gene expression profile and frequently deregulated in
652 cancers. This is the case for *HDAC3*, commonly upregulated in solid tumors (Karagianni and
653 Wong, 2007). In glioma, HDAC3 silencing steers to an impaired 3D tube formation along with
654 a decrease in MMP-14, laminin-5γ2 (the latter likely involved in AKT/ERK activation signaling)
655 (Liu et al., 2015). More generally, pharmacological inhibition of class I and II HDACs (HDAC1-
656 10) in glioma cell lines (with SAHA and MC1568), also affects vascular tube formation. The
657 same holds true for GSCs, albeit at higher concentration (2 to 100-fold depending on the HDAC
658 inhibitor), reflecting their well-known resistance to pharmacological treatments (Pastorino et
659 al., 2019). Bromodomain and extra-terminal domain (BET) proteins are epigenetic decoders
660 that recognize acetylated marks on proteins (including histones) and recruit proteins driving

661 transcriptional activation. JQ1, a BET inhibitor was effective in inhibiting VM of pancreatic
662 ductal adenocarcinoma cells by decreasing the ERK1/2-MMP-2/-9 signaling pathway both *in*
663 *vitro* and *in vivo* (Zhuo et al., 2019).

664 A large body of data report the interleukin-33 (IL-33) and its receptor ST2 (encoded by
665 *IL1RL1*) to be important in tumor immune response and cancer cell invasion. As such the IL-
666 33/ST2 axis is now considered as a promising new immunotherapy (Liew et al., 2016).
667 Recently, IL-33 was shown to promote VM tube formation in aggressive melanoma cell lines.
668 Mechanistically, downstream ST2 IL-33 could trigger the ERK1/2 phosphorylation and MMP-
669 2/-9 expression (Yang et al., 2019). However, even though IL-33 was previously described to
670 induce a migrating mesenchymal phenotype, this aspect was not investigated in the context
671 of VM. LOXL2 also plays a key role in extracellular matrix remodeling and particularly in
672 collagen and elastin fibers stabilization which is involved in several processes including cell
673 adhesion, migration, invasion and the EMT. Particularly, LOXL2 interacts and cooperates with
674 Snail to downregulate E-cadherin expression in metastatic carcinoma (Peinado et al., 2005). It
675 is thus not surprising that LOXL2 was found correlated to VM (and to VE-cadherin expression
676 in cancer cells), metastasis and poor patient prognosis in HCC (Shao et al., 2019).

677

678 *3.7. Semaphorins, potential guides in VM*

679 The Semaphorin family is composed of membrane-anchored and secreted guidance cues
680 which provide a wide repertoire of signals, paramount for neuronal growth, angiogenesis and
681 epithelial barrier integrity (Treps et al., 2013). As such, semaphorins have been linked to EMT
682 in pancreatic (Saxena et al., 2018; Tam et al., 2017), hepatic (Lu et al., 2018; Pan et al., 2016),
683 breast (Yang et al., 2015a), cervical (Song and Li, 2017), ovarian (Tseng et al., 2011), head and
684 neck (Wang et al., 2016) and oral cancers (Liu et al., 2018; Xia et al., 2019). Analogous to the

685 Ephrin guidance molecules described in the aforementioned section, the expression of the
686 membranous Semaphorin-4D is correlated with VM in a cohort of non-small cell lung cancer
687 (NSCLC). Downstream its receptor plexinB1, Semaphorin-4D triggers the RhoA/ROCK pathway
688 thereby promoting cancer cell migration and invasion, and the occurrence of VM *in vitro* and
689 in xenograft model (Xia et al., 2019). Accordingly, previous studies already reported the
690 involvement of the RhoA/ROCK signaling in VM formation in melanoma, osteosarcoma and
691 HCC (Xia et al., 2017; Xia et al., 2015; Zhang et al., 2014b; Zhang et al., 2015a). Semaphorin-
692 4D silencing also led to a reduction in VE-cadherin, EphA2 and MMP-2/-9, suggesting an
693 intertwined relationship between these partners during VM in NSCLC (Xia et al., 2019). In
694 other models of lung adenocarcinoma, downstream the SAV1-MST1/2-LATS1/2-YAP/TAZ axis
695 Semaphorin-4D was also shown to participate in VM formation (Zhao et al., 2020). Moreover,
696 at the surface of head and neck squamous cell carcinoma cell lines, MT1-MMP proteolytically
697 cleaves Semaphorin-4D and induces Semaphorin-4D-dependent pro-angiogenic response in
698 surrounding endothelial cells (Basile et al., 2006). It is thus not farfetched to hypothesize that
699 this phenomenon could also occur between cancer cells, allowing a directional migration
700 during VM network formation.
701
702 *3.8. Notch signaling in VM*
703 The Notch pathway is a highly conserved intercellular signaling. Activated by the interaction
704 of the trans-membrane ligands Delta-like (Dll1-4) and Jagged-1/-2 with Notch receptors
705 (Notch 1-4) expressed on adjacent cells, signal transduction is propagated *via* the γ-secretase-
706 driven proteolytic cleavage of Notch receptor intracellular domain (NICD) that is released and
707 form a nuclear transcriptional activator complex (Bray, 2016). Initial work indicates that Notch
708 1/2, Jagged-1/-2 and Dll1 are upregulated in 'dysplastic nevi' and melanomas as compared to

709 common melanocytic nevi (Massi et al., 2006). Similarly, Notch 4 and Dll4 are overexpressed
710 in aggressive melanoma cell lines where Notch 4 is enriched in melanoma VM networks
711 (Demou and Hendrix, 2008), while Notch 4 blocking antibodies impair VM *in vitro* in a Nodal-
712 dependent manner (NICD can bind and drive Nodal gene expression) (Hardy et al., 2010).
713 Remarkably, Nodal was overexpressed in metastatic melanoma tissues, and curbing
714 downstream signaling pathway (*via* an ALK 4/5/7 inhibitor) could abrogate melanoma cell
715 invasion and tube formation capacity (Topczewska et al., 2006). In breast cancer,
716 overexpression and silencing strategies underline that Nodal promotes VM *via* the Smad2/3
717 pathway (Gong et al., 2016). Additionally, Notch 4 and Dll4 were also found to be associated
718 with VM, metastasis and poor prognosis in NSCLC (Wang et al., 2018). In aggressive human
719 melanoma cell lines, disruption of the Notch signaling with the DAPT γ-secretase inhibitor
720 leads to a seemingly more matured and stabilized *in vitro* tubular network, and melanoma
721 xenografted tumors displays larger and more branched VM channels, associated with an
722 increase in MMP-2 and VEGFR-1 expression (Vartanian et al., 2013). Choriocarcinoma, a rare
723 and highly metastatic gestational trophoblastic cancer, is reported to involve VM with
724 syncytiotrophoblasts lining pseudovascular channels (Shih, 2011), a process that is similar to
725 the embryonic microcirculatory networks (Rai and Cross, 2014). Forskolin is an inducer of
726 syncytiolization, and Forskolin treatment in choriocarcinoma cells resulted in high expression
727 of the VM markers MMP-2/-9, EphA2 and VE-cadherin, tube formation, as well as the
728 activation of the Notch 1 signaling pathway. However, invasive ability and VM markers were
729 reversed by DAPT, suggesting a mechanism whereby Notch-signaling down tunes VM in
730 choriocarcinoma (Xue et al., 2020). Notwithstanding the behavior of trophoblasts is similar to
731 aggressive tumors during differentiation and implantation (Rai and Cross, 2014), Notch 1

732 signaling seems to have an opposing effect in melanoma and NSCLC (Vartanian et al., 2013;
733 Wang et al., 2018), calling for further investigations before therapeutic applications.
734
735 *3.9. COXs inflammation in VM*
736 COX-2 is an enzyme responsible for catalyzing the conversion of arachidonic acid into
737 prostaglandins such as PGE2, of paramount importance during inflammation. Subsequently,
738 PGE2 binding to the prostaglandin E2 receptor subtypes (EP1-4) activates the EGFR signaling,
739 and PKC-dependent ERK1/2 activation, pathways described to be involved in VM (Fig. 3A). In
740 breast cancer, COX-2 expression correlates directly with aggressiveness and metastasis. As
741 such, *in vitro* VM tube formation is largely impaired by celecoxib treatment, a selective COX-
742 2 inhibitor, but nearly completely rescued when cells are supplemented with prostaglandin
743 E2. Unbiased bulk RNA-sequencing approach was followed to disentangle the underlying
744 regulatory mechanism. Interestingly, genes related to angiogenesis (e.g. MMP-1, fibronectin,
745 LAMC2) and proliferation (STAT1, EGFR, MAPK) were diminished. Protein array further
746 validated a reduction in major angiogenic proteins such as VEGF and TIMP-1/-2, making a
747 parallel between VM and angiogenic pathways (Basu et al., 2006). Treatments with specific E2
748 receptor antagonists further highlight the involvement of the EP3 and EP4 receptors to
749 mediate the aggressive phenotype of SUM149 and SUM190 inflammatory breast cancer cells,
750 and mediate VM 3D tube formation (Robertson et al., 2010). Of note, in glioblastoma, the
751 presence of VM channel is associated with the expression of COX-2 and MMP-9 (Liu et al.,
752 2011b). In an elegant *in vitro* coculture model of U87 glioma cell line and IL-4-activated M2
753 macrophages (as a model of TAMs), tube formation and COX-2 expression were increased.
754 Downstream COX-2, the PGE2/EP1/PKC pathway was of prime importance to induce VM

755 formation, and further confirmed *in vivo* with COX2-deficient U87 xenograft model (Rong et
756 al., 2016).
757
758 *3.10. Non-coding RNAs*
759 Non-coding RNAs (ncRNAs) are not translated into proteins but bear a remarkable variety of
760 biological functions such as RNA processing, transcription and translation regulations. ncRNAs
761 can be grouped according to their length with long non-coding RNAs (lncRNAs) exceeding 200
762 nucleotides in length, small non-coding RNAs between 200 and 50 nucleotides, and tiny
763 ncRNAs for the smallest. The latest group includes siRNAs, miRNAs and piRNAs. In this section,
764 we summarized the mechanistic insights of ncRNAs involved during the process of VM (Table
765 1). For ease of reading, the different ncRNAs are mostly discussed and grouped by tumor
766 type.
767 Similar to melanoma where VM was initially described (Maniotis et al., 1999),
768 aggressive but not poorly invasive triple negative breast cancer cells, efficiently undergo
769 matrix-associated VM under hypoxia. Upon transfection with miR-204, VM tube formation
770 was highly impaired. The pleiotropic effect of the miRNA was assessed using ELISA-based
771 phosphorylation antibodies arrays that revealed a reduced expression and phosphorylation
772 levels of 13 proteins involved in PI3K/AKT, RAF1/MAPK, VEGF, and FAK/SRC signaling.
773 Subsequent validation studies using inhibitors confirmed that PI3K-α and c-SRC signaling were
774 a requisite for VM, and impeded by miR-204 (Lozano-Romero et al., 2020; Salinas-Vera et al.,
775 2018). The lncRNA TP73-AS1 was found upregulated in VM positive tissues from triple
776 negative breast cancer (Tao et al., 2018). Twist1, that accelerates tumor cell VM in breast
777 cancer (Zhang et al., 2014a) harbors a potential miR-490-3p binding site. Tao et al. showed
778 that TP73-AS1 inhibition could release the post-translational suppression of Twist1 induced

779 by miR-490-3p, and thus precluded VM formation (Tao et al., 2018). Interestingly, miR-490-
780 3p was also identified to be play a role in clear cell renal cell carcinoma. Particularly, the
781 NR2C2 (nuclear receptor subfamily 2 group C member 2; aka TR4) could repress the miR-490-
782 3p-dependent vimentin inhibition, and thus favor VM, tumor growth and metastasis (Bai et
783 al., 2018). Dimethylarginine dimethylaminohydrolase 1 (DDAH1) is responsible for the
784 conversion of asymmetric dimethylarginine (ADMA) to citrulline. ADMA is an endogenous
785 inhibitor of the nitric oxide synthase (NOS) and plays a key role in angiogenesis (Eelen et al.,
786 2018). In aggressive breast cancer cell lines, DDAH1 overexpression was counteracted by miR-
787 193b which further disrupted VM (Hulin et al., 2017). The miR-124 was previously shown to
788 inhibit EMT and breast cancer metastasis by targeting Slug (Liang et al., 2013). A report
789 indicates that in cervical cancer, miR-124 down-regulates VM, migration and invasion, as a
790 result from its interaction with AmotL1, a member of the angiomotin family that regulates
791 cell growth and motility.

792 A recent study identified 11 miRNAs that are differently expressed by the SKOV3
793 ovarian cancer cell line during tube formation in an hypoxic environment. Among the so-
794 called "hypoxamiRs", miR-765 was deeply downregulated upon hypoxia, and could decrease
795 the levels of AKT/SRC axis and exert a negative regulation on VEGF-A by specific binding to its
796 3'UTR (Salinas-Vera et al., 2019). This time without any link to hypoxia, miR-200a expression
797 was significantly lower in VM positive ovarian cancer. *In vitro* works indicate that it miR-200a
798 and miR-27b negatively regulates EphA2 and VE-cadherin expression, respectively, and thus
799 inhibits VM (Liu et al., 2017; Sun et al., 2014).

800 Expression of the lncRNA LINC00312 is found to be higher in lung adenocarcinoma
801 patients with metastasis. Seemingly, mice inoculated with LINC00312-overexpressing
802 adenocarcinoma cells presented more lung metastatic tumor nodules and higher VM. RNA

803 pull-down assay identifies YBX1 as the sole interacting partner with LINC00312, that allows
804 the increased expression of VE-cadherin, TGF-β, VEGF-A/-C levels putatively *via* AKT
805 activation (Peng et al., 2018). Oncogenic signaling downstream estrogen receptor beta (ERβ)
806 play an important role in NSCLC progression and EMT. Particularly, ERβ activation up-
807 regulates MALAT1 expression and thus prevent miR-145-5p-mediated NEDD9
808 downregulation. In this setup, the oncogene NEDD9 seems primordial in inducing VM and cell
809 invasion (Yu et al., 2019). MALAT1 expression was also tightly associated with VM in gastric
810 cancer, via the induction of several signaling pathways including VE-cadherin/β-catenin
811 complex, ERK/MMP and FAK/paxillin signaling (Li et al., 2017b). Investigating whether these
812 pathways are also affected during NSCLC-associated VM would be interesting.

813 It was shown that c-Myc and SOX2 are important to maintain the pool of liver CSCs,
814 and also to induce VM (Sun et al., 2013). As such, when c-Myc and SOX2 were co-transduced
815 in the HCC cell line HepG2, these cells displayed increased migration, invasion and 3D tube
816 formation properties (Zhao et al., 2018). When compared to HepG2 parental cells, unbiased
817 bulk RNA-sequencing identified 748 differentially expressed ncRNAs, among which lncRNA
818 n339260 that was enriched in the c-Myc/SOX2 overexpressing cells. LncRNA n339260
819 overexpression in HepG2 was able to promote VM (higher VE-cadherin expression) and CSC
820 markers, and VM tube formation. The miR-31-3p, miR-30e-5p, miR-520c-5p, miR-519c-5p,
821 and miR-29b-1-5p were considered to be downstream the lncRNA n339260 (or regulated by
822 the latter) as their expression increased/decreased following lncRNA n339260
823 upregulation/downregulation respectively (Zhao et al., 2018). In colorectal cancer, SOX2 is
824 also important for maintaining CSC properties. Ectopic overexpression of miR-450a-5p was
825 shown to suppress the expression of SOX2 by targeting its 3' UTR region and hence restrained
826 SOX2-induced CSC properties, angiogenesis, and VM (Chen et al., 2020). Yang *et al*. studied

827 the mechanism of VM formation in the context of HCC tumor cells and CAF communication.
828 While CAF-secreted TGF-ß and SDF1 promote VM formation in tumor cells, miR-101 could
829 attenuate TGF-ß signaling by targeting its receptor TGF-ßR1 and the downstream effector
830 Smad2 in tumor cells, and simultaneously abrogate SDF1 expression in CAFs. miR-101 is thus
831 pivotal to extinguish VM-promoting signaling in two different cell types (Yang et al., 2016).
832 Zhao et al. found that miR-27a-3p expression was inversely associated with Twist1
833 expression. miR-27a-3p appears to mediate the inhibition of EMT and VM by downregulating
834 VE-cadherin (upon binding to its 3'UTR), and miR-27a-3p down-regulation is associated with
835 metastasis (Zhao et al., 2016a). miR-186 also suppresses Twist1 expression in prostate cancer,
836 and hence thwarted EMT, cell motility and tube formation *in vitro* and metastasis in mouse
837 model (Zhao et al., 2016b).
838 So far, glioma is the tumor entity with the greatest variety of miRNAs and lncRNAs
839 described to play a role in VM. miR-Let-7f halted VM by disturbing periostin-induced
840 migration of glioma cells (Xue et al., 2016). The levels of miR-141 (Li et al., 2018a), miR-26b
841 (Wu et al., 2011) were inversely correlated with the grade of glioma, and both miRNAs were
842 shown to directly target EphA2 an important regulator in VM. Recently, the group of Prof.
843 Xue has studied two lncRNAs (LINC00339 and HOXA-AS2) that are upregulated in human
844 glioma and positively correlated to VM. LINC00339 binds and prevents the action of the miR-
845 539-5p, thereby activating the Twist1/MMP-2/MMP-14 signaling pathway to promote VM
846 (Guo et al., 2018) (Fig. 3B). HOXA-AS2 acts via a different pathway, which first involves its
847 binding to miR-373. Downstream EGFR signaling, miR-373 regulates the expression of VE-
848 cadherin, MMP-2/-9 and thus VM (Gao et al., 2018). Stathmin 1 is a member of the
849 microtubule destabilizing protein family that regulates microtubule dynamics during cell-
850 cycle progression. Stathmin 1 is overexpressed in various cancers and its expression is

851 positively associated with higher grades of human glioma. In glioma cell lines, stathmin 1
852 appears to be the target of the (central nervous system) tissue specific miR-9 that refrains
853 growth and VM of ectopic xenografts (Song et al., 2013). Interestingly, over-expression of
854 miR-584-3p paralyses hypoxia-induced VM formation in human A172 glioma cells, by
855 antagonizing ROCK1-dependent stress fiber formation (Xu et al., 2017). As mentioned before,
856 the RhoA/ROCK signaling pathway has been described to participate in VM formation in
857 melanoma, osteosarcoma and HCC (Xia et al., 2017; Xia et al., 2015; Zhang et al., 2014a; Zhang
858 et al., 2015b). Recently, three studies from the same group identified several lncRNAs
859 regulating VM in glioma. Important translational regulations occur from the 3' and 5'
860 untranslated regions (UTR) of mRNAs. Particularly, upstream open reading frames (uORFs),
861 commonly found in the 5'UTR of eukaryotic genes, are important in the initiation of
862 translation. uORFs in a gene initiate nonsense-mediated RNA decay (NMD) that promotes
863 transcript degradation. An uORF was identified in the lncRNA ZNRD1-AS1, namely ZNRD1-
864 AS1-144aa-uORF. ZNRD1-AS1 is highly expressed in glioma and promotes VM formation,
865 while 144aa-uORF was down-regulated and VM hindered. Mechanistically, the lncRNA
866 ZNRD1-AS1 binds to miR-499a-5p, which in turn regulates the ELF1/EMI1 axis to hamper VM
867 formation (Wang et al., 2020a). Therefore, via an intricate regulatory process, the lncRNA
868 ZNRD1-AS1 could foster VM in glioma. The human splicing factor zinc finger, Ran-binding
869 domain containing protein 2 (ZRANB2) is a splicing protein that is part of the
870 supraspliceosome and mediates differential splicing of numerous primary transcripts (Yang
871 et al., 2013). The lncRNA SNHG20 is correlated with poor overall survival and tumor-node-
872 metastasis in several cancer types. In glioma cells, ZRANB2 promoted VM formation by
873 increasing SNHG20 stability. As a consequence, SNHG20 was able to promote Forkhead box
874 K1 degradation, thereby alleviating the transcriptional inhibition of VM-related proteins

875 MMP-1/-9 and VE-cadherin (Li et al., 2019). Hence, TZRANB2 and SNHG20 were powerful
876 inducers of VM formation in glioma. Another recent report studied the regulation of the
877 poly(A) binding protein cytoplasmic 5 (PABPC5), which binds to the 30 end of the poly(A) tail
878 of most eukaryotic mRNAs. Interestingly, overexpression of the lncRNA HCG15 or PABPC5
879 promoted VM, while upregulation of the transcriptional repressor ZNF331 greatly curbed VM
880 by directly repressing LAMC2 (coding for Laminin-5γ2, important for VM (Seftor et al., 2001;
881 Sood et al., 2001)) and PABPC5 transcription. By targeting the VM-inhibitor ZNF331, the
882 lncRNA HCG15 could thus promote VM formation in glioma (Jing et al., 2020).
883 In conclusion, these studies highlight the complexity and diversity of VM-related
884 processes regulated by lncRNAs and miRNAs (Table 1). To our knowledge, presently no study
885 reports the direct implication of EVs during VM. However, these EVs are recognized carriers
886 of several ncRNAs and also modulators of extracellular matrix remodeling, a process greatly
887 involved during VM. As a proof-of-concept, using the user-friendly online EVmiRNA database
888 (Liu et al., 2019), we could identified miR-450a-5p and miR-101-3p as expressed in EVs from
889 colon carcinoma (with a preferential enrichment in microvesicles). As such, in-depth
890 investigations of the implication of EVs and EV-carried ncRNAs may certainly warrant
891 interesting findings in VM formation.
892
893 **4. VM and cancer therapy**
894 *4.1. Cancer resistance*
895 For many aggressive tumors, current therapeutic strategies are insufficient. Thus, VM
896 formation could explain the therapeutic resistances observed with cytotoxic or targeted
897 chemotherapies: residual tumor cells may form VM channels, thereby providing oxygen and
898 nutrients, which support cell proliferation and cancer progression. Not only has VM been

899 reported in different solid tumors, but tumor cell-originated neovascularization including
900 tumor-derived endothelial cell-induced angiogenesis along with VM have been suggested to
901 be involved in the development of resistance to anti-VEGF therapy as frequently observed in
902 glioblastoma. Anti-angiogenic drugs, mostly affecting VEGF-VEGFR pathway, cause dramatic
903 tumor size reduction and are largely used in glioblastoma therapy as adjuvants to control
904 abnormal vasculature. However, the benefits are transient since glioblastoma rapidly show
905 resistance to anti-angiogenic therapies upon prolonged treatment through the activation of
906 alternative vascularization pathways (Angara et al., 2017; Arbab et al., 2015). Moreover, it has
907 been noted that hypoxia associated with anti-angiogenic therapies may induce VM that
908 represents a mechanism whereby glioblastoma can escape anti-angiogenic therapies (Angara
909 et al., 2017). VM is also reported to represent a non-angiogenic pathway in breast-cancer
910 metastasis. In this last tumor, it has been reported that angiogenic primary breast carcinoma
911 can relapse not only as angiogenic, but also as non-angiogenic lung metastases. The authors
912 propose that this non-angiogenic pathway is a novel pathway of cancer progression and such
913 tumors are likely to be resistant to anti-angiogenic treatment. In addition, the role of anti-
914 angiogenic treatment in VM promotion has been confirmed in a study conducted in triple-
915 negative breast cancer cells. Thus, an enhancement of VM-positive cases has been observed
916 in sunitinib (a VEGFR tyrosine kinase inhibitor)-treated cells in comparison with control cells.
917 These effects were explained by an overexpression of HIF-1α, VE-cadherin and Twist1 (Sun et
918 al., 2017). More recently, a study has been conducted with trastuzumab, a drug that target
919 the receptor tyrosine kinase HER2 in breast cancer cells. Several VM markers were
920 upregulated in trastuzumab-treated cells suggesting that HER-2 positive breast cancer cells
921 can exhibit VM in an angiogenic microenvironment after acquiring trastuzumab resistance

922 (Hori et al., 2019). Hence, VM may be regarded as one of the major causes of the development
923 of resistance to anti-angiogenic therapy in solid tumors.
924
925 *4.2. Therapeutic targeting of VM*
926 If it is clearly established that VM participates in the therapeutic resistances of many solid
927 tumors, in this regards it constitutes a promising reservoir for developing novel anticancer
928 therapeutics, and an armamentarium of drugs has been investigated (Table 2). Recently,
929 studies have been conducted with histone deacetylase (HDAC) inhibitors both in glioblastoma
930 and in aggressive triple-negative breast cancer. As previously described, altered expression
931 and/or function of HDAC could play an important role in tumor initiation and progression (Li
932 et al., 2018b) and these enzymes are promising therapeutic targets in various cancers (Sun et
933 al., 2018).
934 Interestingly, *in vitro* and *in vivo* evidences suggested the antitumor activity of HDAC
935 inhibitors by preventing VM in different cancer models. For instance, it has been found that
936 vorinostat, trichostatin A, entinostat (MS275) and MC1568 significantly decrease tube
937 formation by U87MG and GSCs. These results were explained, at least in part, by a significant
938 decrease of migration and invasion of glioma cells upon HDAC treatments (Pastorino et al.,
939 2019). Furthermore, it has been reported that the specific HDAC inhibitor, entinostat, is able
940 to reduce VM structure formations in various triple-negative breast cancer cells. Thus, this
941 study revealed that treatment of MDA-MB-231, LM2-4, BT-549 or MCF-7 with entinostat
942 epigenetically led to the re-expression of the anti-angiogenic genes, serpin family F member
943 1 (SERPINF1) and thrombospondin 2 (THBS2), as well as the tumor suppressor genes,
944 phosphatase and tensin homolog (PTEN) and p21. Otherwise, it has been found that
945 entinostat downregulated the expression of VEGF-A, and that of the EMT-related genes,

946 vimentin and β-catenin (Maiti et al., 2019). These two studies offer interesting perspectives
947 for the use of HDAC inhibitors against VM. However, these studies have limited clinical
948 translation as they lack to evaluate the impact of these molecules on VM formation *in vivo*.
949 No pre-clinical or clinical studies have yet been considered with HDAC inhibitors and it is still
950 too early to seriously envision these molecules as potential therapeutic agents against VM
951 formation.

952 As previously described, CSCs are main actors in VM formation and are also responsible
953 for the low survival rate of patients with aggressive tumors. After chemo- and radiotherapy,
954 only a small proportion of CSCs are capable to induce recurrence. Furthermore, EMT is also
955 involved in the acquisition of CSC properties. Taken together, these findings suggest that a
956 combination of EMT and CSC targeting may be beneficial for anti-VM formation therapy
957 through a decrease of both invasion and metastasis and an improvement of patient's survival
958 rate. It has been found that salinomycin, a potassium ionophore used as an anticoccidial drug,
959 completely suppressed VM. The most prominent property of this drug is that it selectively kills
960 CSCs (Gupta et al., 2009).

961 Furthermore, because VEGF-A enhances the ability of melanoma cells to form tube-
962 like structures by activating VEGFR-1 and the downstream PKC-α pathway, it has been
963 suggested to target VEGFR-1 to prevent VM (Fig. 3A). Interestingly, an anti-VEGFR-1
964 monoclonal antibody (D16F7) has shown antitumor activity by inhibiting chemotaxis,
965 extracellular matrix invasion and VEGFR-1^{+} cancer cells VM in melanoma and glioblastoma,
966 two aggressive tumors (Atzori et al., 2017; Graziani et al., 2016). Taken together, these
967 findings highlight tumor type specificities and could explain the limited efficacy of sorafenib
968 and thus suggesting a therapeutic benefit for tyrosine kinase inhibitors targeting preferentially
969 VEGFR-1.

970 Various other strategies have been under discovery to inhibit VM formation. Because
971 MMP-2- and MT1-MMP-mediated laminin-γ2 cleavage reportedly induces VM formation, anti-
972 MMP-2 or anti-MT1-MMP blocking antibodies treatment has been proposed to abrogate it
973 (Seftor et al., 2001). A similar outcome was achieved when treating 3D culture of ovarian
974 cancer cells at the onset of tube formation with incyclinide (*aka* Metastat), an inhibitor of
975 MMP activity. However, this treatment could not affect an established network, suggesting a
976 role of MMPs in early steps of tube formation rather than for their stability (Sood et al., 2001).
977 A derivative of incyclinide has made it to the clinics with COL-3 (NSC-683551) to treat patients
978 with refractory metastatic cancers (NCT00001683).
979 In addition, nanostructured functional drug-loaded liposomes, modified with an HIV
980 peptide lipid-derivative conjugate and containing the chemotherapeutics epirubicin and
981 celecoxib were tested for their effect on VM. The added value of this delivery system was to
982 improve pharmacokinetic properties and bio-distribution of such anticancer agents. As such,
983 tail vein injection of drug-loaded liposomes reduced VM expression via the inhibition of VE-
984 cadherin, FAK, EphA2, HIF-1α, and MMP-9 in invasive breast cancer xenografts in nude mice
985 (Ju et al., 2014). Doxycycline has been used in combination with targeted drugs in clinical trials
986 for patients with advanced cancer. Doxycycline is a semi-synthetic tetracycline which can
987 inhibit MMP activation and cell proliferation, as well as interfere with tumor-related protein
988 synthesis in mammalian cells. Doxycycline has a strong inhibitory effect on malignant cells
989 especially NCI-H446 and A549 lung cancer cells (Cao et al., 2013; Ko et al., 2015). Interestingly,
990 doxycycline treatment prolonged the mouse survival time and partly suppressed the growth
991 of engrafted HCC tumor cells, with an inhibition rate of 43.39% (Meng et al., 2014). In HCC and
992 lung cancer models, doxycycline is capable to inhibit E-cadherin degradation and down-
993 regulates the expression of vimentin protein (Cao et al., 2013; Ko et al., 2015; Meng et al.,

994 2014). These findings show that doxycycline acts upstream of EMT-related signal transduction
995 to inhibit a wide range of cellular function. As such, investigations in HCC revealed that (i) *in*
996 *vitro* doxycycline promoted cell adhesion but hampered HCC cell viability, proliferation,
997 migration and invasion; and (ii) *in vivo* higher amounts of VM and endothelium-dependent
998 vessels were found in the control group than the treatment group (Meng et al., 2014).

999 Among the new molecules used in antitumor therapies, encouraging results have been
1000 obtained with galunisertib (LY2157299), a selective ATP-mimetic inhibitor of TGF-βR1, that
1001 improved glioma prognosis. Thus, from *in vitro* and pre-clinical studies, it has been found that
1002 VM was inhibited by galunisertib through a decrease in VE-cadherin and αSMA expression, as
1003 well as down-regulation of AKT and VEGFR-2 phosphorylation in galunisertib-treated glioma
1004 cells (Zhang et al., 2016).

1005 Recently, several studies involving molecules extracted from plants have been tested
1006 in different tumor models. The properties of brucine, a traditional medicinal herb extracted
1007 from seeds of *Strychnos nux-vomica* have been tested in a triple-negative breast cancer cell
1008 line MDA-MB-231. The authors concluded that brucine inhibited VM through repressing
1009 EphA2 and MMP-2/-9 expression (Xu et al., 2019). Another study evaluated the effects of
1010 polyphyllin I, the main component of *Rhizoma paridis* in VM in HCC. It has been reported that
1011 polyphyllin I blocked VM through an inhibition of PI3K/AKT – Twist1 – VE-cadherin axis
1012 through a regulation of the transcriptional activity of Twist1 (Xiao et al., 2018). In a B16F10
1013 metastatic melanoma model, Bhattacharyya *et al*. proposed lupeol as a substitute for
1014 dacarbazine at the onset of therapeutic resistance because it is able to block VM through a
1015 downregulation of the CSC marker CD133 (Bhattacharyya et al., 2019). If the abovementioned
1016 studies seem exciting for their authors, they remain extremely preliminary and do not
1017 constitute (yet) alternatives to recognized therapies. Indeed, no precise pharmacological data

1018 has been demonstrated for the different molecules tested. The works do not specify the
1019 pharmacodynamic or pharmacokinetic characteristics of these molecules. For instance,
1020 brucine is weakly liposoluble (Li and Wang, 2017) and hardly crosses the barrier formed by the
1021 plasma and nuclear membranes. Also, if the pharmacological targets are intracellular, its
1022 availability may be limited. In addition, in the case of lupeol, the doses used to block VM are
1023 very high (40 mg/kg) and the published data did not provide clear evidence of a true antitumor
1024 activity of this molecule. According to our previous work (Pautu et al., 2019), the mice model
1025 B16F10 is extremely aggressive and, for us, it is not possible to think that lupeol is sufficient
1026 by itself to limit the progression of this metastatic melanoma.
1027

1028 **5. Conclusion**

1029 As highlighted above, a plethora of signaling pathways and multiple growth factors and their
1030 receptors are described to promote VM. Therefore, one could predict that hindering a single
1031 signaling pathway by means of an inhibitor would have a limited suppressive effect on VM,
1032 since other signaling pathways would immediately compensate and eventually restore the
1033 process of switching to VM phenotype. In fact, inhibitors such as galunisertib, LY294002 (a
1034 PI3K inhibitor), doxycycline, everolimus or regorafenib showed only limited efficacy. For
1035 several months, it has been recognized that therapeutic combinations are essential to treat
1036 aggressive cancers. Therefore, it is essential to increase the number of studies combining
1037 different therapeutic approaches in order to limit tumor development by blocking significantly
1038 VM formation.
1039

1040 **Declaration of Competing Interest**

1041 The authors declare no conflict of interest.

1042

1043 **Acknowledgements**

1044 L.T. is supported by the Research Foundation Flanders (FWO), and the NExT Junior Talent

1045 Initiative.

1046

1047 **Figure legends**

1048 **Table 1. Non-coding RNAs involved during vasculogenic mimicry**

1049 TNBC: triple negative breast cancer; HCC: Hepatocellular carcinoma.

1050

1051 **Table 2. Summary of therapeutics targeting vasculogenic mimicry**

1052 CSCs: Cancer stem cells; GSCs: Glioblastoma stem cells; HCC: Hepatocellular carcinoma.

1053

1054 **Fig. 1. The two types of vascular mimicry.**

1055 **A)** Patterned vasculogenic mimicry (VM) forms architectural patterns of loops and networks

1056 as revealed by periodic acid-Schiff (PAS)-stained phase contrast micrograph of metastatic

1057 cutaneous melanoma C8161 3D culture. Pictures acquire after 1 week on Matrigel;

1058 magnification x40. **B)** Tubular VM showing melanoma cancer cells that lined a vascular channel

1059 containing red blood cells, but without endothelial cells identified. Hematoxylin-eosin-

1060 staining; magnification x100. Reprinted from "Vascular Channel Formation by Human

1061 Melanoma Cells in Vivo and in Vitro: Vasculogenic Mimicry" by Maniotis et al., The American

1062 Journal of Pathology, 155/3, 739-752, 1999, with permission from Elsevier.

1063

1064 **Fig. 2. Partners in crime during vasculogenic mimicry in tumors.**

1065 Tumor vascularization can be achieved by several processes such as the classical endothelium-
1066 dependent sprouting angiogenesis vasculogenic (bottom right), and endothelium-
1067 independent tubular vasculogenic mimicry (VM). Such blood conducting network is built by
1068 cancer cells themselves resting on an extracellular matrix (ECM) rich in laminin, stained by
1069 periodic acid Schiff (PAS; depicted as the red outline) without endothelial markers such as
1070 CD31 or CD34. In the tumor microenvironment, various cell types foster VM network
1071 formation. (i) The epithelial-mesenchymal transition (EMT) whereby cancer cells lose their
1072 polarity and acquire a migratory mesenchymal phenotype upon several signaling pathways
1073 (TGF-ß, Wnt, Notch, etc.) and transcription factors (Snail, Twist1, ZEB1/2). (ii) Cancer
1074 associated fibroblasts (CAFs) are important player in ECM remodeling and their secretome
1075 contribute to VM formation. (iii) Tumor associated macrophages (TAMs) contribute to cancer
1076 cell transdifferentiation and pro-inflammatory cytokines. (iv) Cancer stem cells (CSCs) harbor
1077 pluripotent features allowing them to differentiate and form VM network, but also to do
1078 endothelial transdifferentiation contributing to tumor angiogenesis.
1079
1080 **Fig. 3. Molecular highlights involved during vasculogenic mimicry formation.**
1081 **A)** VEGF-A, downstream the activation of VEGFR-1, lead to the activation of the PI3K/PKC
1082 pathway, converging to AKT with actin reorganization, and thus promoting vasculogenic
1083 mimicry (VM). COX-2 transforms the arachidonic acid into prostaglandin E2 (PGE2) that acts
1084 on its receptor E2 to foster the PKC/ERK1/2 axis, important during VM. Endothelin, via its
1085 receptor EDNRB, leads to ß-arrestin-mediated c-SRC activation, which in turn cooperates with
1086 VEGF-C/-D to phosphorylate VEGFR-3. The VEGFR-3 activation leads to MMP2 transcription
1087 into its pro-MMP-2 form that require proteolytic activation from the MT1-MMP/TIMP2
1088 complex. The active MMP-2 can then trigger the cleavage of laminin-ɣ2 into laminin-5ɣ2',

1089 which stimulates VM. **B)** Downstream VEGF-1/VEGFR-2 or EphA2 receptors, VE-cadherin can
1090 be phosphorylated on its tyrosine 658 (Y658) by FAK. Downstream PI3K/AKT and ERK
1091 activation, the expression of several MMPs (MMP-14/-2/-9) is induced and will activate the
1092 MMP-2-mediated VM functions in a similar manner as described for MT1-MMP. Via pY658,
1093 FAK mediates VE-cadherin nucleus translocation and the VE-PTP/p120 complex appears
1094 important to control this process. In the nucleus, upon binding to p120, the transcription
1095 repressor Kaiso can no longer repress the VM-inducible genes CCND1 and WNT11. When
1096 cancer cells are cultured on a matrix coated with the extracellular domain of VE-cadherin, the
1097 EphA2 and PI3K/AKT pathways are activated, and VM formation initiated.

1098

1099 **References**

1100 Aghajani, M., Mokhtarzadeh, A., Aghebati-Maleki, L., Mansoori, B., Mohammadi, A., Safaei, S.,
1101 Asadzadeh, Z., Hajiasgharzadeh, K., Khaze Shahgoli, V., and Baradaran, B. (2020). CD133
1102 suppression increases the sensitivity of prostate cancer cells to paclitaxel. Mol Biol Rep *47*,
1103 3691-3703.
1104 Angara, K., Rashid, M. H., Shankar, A., Ara, R., Iskander, A., Borin, T. F., Jain, M., Achyut, B. R.,
1105 and Arbab, A. S. (2017). Vascular mimicry in glioblastoma following anti-angiogenic and anti-
1106 20-HETE therapies. Histol Histopathol *32*, 917-928.
1107 Arbab, A. S., Jain, M., and Achyut, B. R. (2015). Vascular Mimicry: The Next Big Glioblastoma
1108 Target. Biochem Physiol *4*.
1109 Atzori, M. G., Tentori, L., Ruffini, F., Ceci, C., Lisi, L., Bonanno, E., Scimeca, M., Eskilsson, E.,
1110 Daubon, T., Miletic, H.*, et al.* (2017). The anti-vascular endothelial growth factor receptor-1
1111 monoclonal antibody D16F7 inhibits invasiveness of human glioblastoma and glioblastoma
1112 stem cells. Journal of experimental & clinical cancer research : CR *36*, 106.
1113 Bai, J., Yeh, S., Qiu, X., Hu, L., Zeng, J., Cai, Y., Zuo, L., Li, G., Yang, G., and Chang, C. (2018). TR4
1114 nuclear receptor promotes clear cell renal cell carcinoma (ccRCC) vasculogenic mimicry (VM)
1115 formation and metastasis via altering the miR490-3p/vimentin signals. Oncogene *37*, 5901-
1116 5912.
1117 Bao, Z., Cheng, Z., and Chai, D. (2018). The expressions of CD133, ALDH1, and vasculogenic
1118 mimicry in osteosarcoma and their clinical significance. Int J Clin Exp Pathol *11*, 3656-3663.
1119 Basile, J. R., Castilho, R. M., Williams, V. P., and Gutkind, J. S. (2006). Semaphorin 4D provides
1120 a link between axon guidance processes and tumor-induced angiogenesis. Proc Natl Acad Sci
1121 U S A *103*, 9017-9022.
1122 Basu, G. D., Liang, W. S., Stephan, D. A., Wegener, L. T., Conley, C. R., Pockaj, B. A., and
1123 Mukherjee, P. (2006). A novel role for cyclooxygenase-2 in regulating vascular channel
1124 formation by human breast cancer cells. Breast Cancer Res *8*, R69.

1125 Bhattacharyya, S., Mitra, D., Ray, S., Biswas, N., Banerjee, S., Majumder, B., Mustafi, S. M., and
1126 Murmu, N. (2019). Reversing effect of Lupeol on vasculogenic mimicry in murine melanoma
1127 progression. Microvasc Res *121*, 52-62.
1128 Bittner, M., Meltzer, P., Chen, Y., Jiang, Y., Seftor, E., Hendrix, M., Radmacher, M., Simon, R.,
1129 Yakhini, Z., Ben-Dor, A.*, et al.* (2000). Molecular classification of cutaneous malignant
1130 melanoma by gene expression profiling. Nature *406*, 536-540.
1131 Bray, S. J. (2016). Notch signalling in context. Nat Rev Mol Cell Biol *17*, 722-735.
1132 Bussolati, B., Bruno, S., Grange, C., Ferrando, U., and Camussi, G. (2008). Identification of a
1133 tumor-initiating stem cell population in human renal carcinomas. FASEB J *22*, 3696-3705.
1134 Bussolati, B., Grange, C., Sapino, A., and Camussi, G. (2009). Endothelial cell differentiation of
1135 human breast tumour stem/progenitor cells. J Cell Mol Med *13*, 309-319.
1136 Cao, J., Song, Y., Bi, N., Shen, J., Liu, W., Fan, J., Sun, G., Tong, T., He, J., Shi, Y.*, et al.* (2013).
1137 DNA methylation-mediated repression of miR-886-3p predicts poor outcome of human small
1138 cell lung cancer. Cancer Res *73*, 3326-3335.
1139 Cao, W., Xu, C., Li, X., and Yang, X. (2019). Twist1 promotes astrocytoma development by
1140 stimulating vasculogenic mimicry. Oncol Lett *18*, 846-855.
1141 Carmeliet, P., and Jain, R. K. (2011). Principles and mechanisms of vessel normalization for
1142 cancer and other angiogenic diseases. Nat Rev Drug Discov *10*, 417-427.
1143 Carmeliet, P., Lampugnani, M. G., Moons, L., Breviario, F., Compernolle, V., Bono, F., Balconi,
1144 G., Spagnuolo, R., Oosthuyse, B., Dewerchin, M.*, et al.* (1999). Targeted deficiency or cytosolic
1145 truncation of the VE-cadherin gene in mice impairs VEGF-mediated endothelial survival and
1146 angiogenesis. Cell *98*, 147-157.
1147 Chen, J., Chen, S., Zhuo, L., Zhu, Y., and Zheng, H. (2020). Regulation of cancer stem cell
1148 properties, angiogenesis, and vasculogenic mimicry by miR-450a-5p/SOX2 axis in colorectal
1149 cancer. Cell Death Dis *11*, 173.
1150 Chen, K. J., Li, Q., Wen, C. M., Duan, Z. X., Zhang, J. Y., Xu, C., and Wang, J. M. (2016). Bleomycin
1151 (BLM) Induces Epithelial-to-Mesenchymal Transition in Cultured A549 Cells via the TGF-
1152 β/Smad Signaling Pathway. J Cancer *7*, 1557-1564.
1153 Chen, Q., Lin, W., Yin, Z., Zou, Y., Liang, S., Ruan, S., Chen, P., Li, S., Shu, Q., Cheng, B., and Ling,
1154 C. (2019). Melittin Inhibits Hypoxia-Induced Vasculogenic Mimicry Formation and Epithelial-
1155 Mesenchymal Transition through Suppression of HIF-1α/Akt Pathway in Liver Cancer. Evid
1156 Based Complement Alternat Med *2019*, 9602935.
1157 Chen, X., and Song, E. (2019). Turning foes to friends: targeting cancer-associated fibroblasts.
1158 Nat Rev Drug Discov *18*, 99-115.
1159 Chiu, D. K., Zhang, M. S., Tse, A. P., and Wong, C. C. (2019). Assessment of Stabilization and
1160 Activity of the HIFs Important for Hypoxia-Induced Signalling in Cancer Cells. Methods Mol Biol
1161 *1928*, 77-99.
1162 Delgado-Bellido, D., Bueno-Galera, C., López-Jiménez, L., Garcia-Diaz, A., and Oliver, F. J.
1163 (2020). Endothelial Phosphatase VE-PTP Participates in Vasculogenic Mimicry by Preventing
1164 Autophagic Degradation of VE-Cadherin. Front Oncol *10*, 18.
1165 Delgado-Bellido, D., Fernández-Cortés, M., Rodríguez, M. I., Serrano-Sáenz, S., Carracedo, A.,
1166 Garcia-Diaz, A., and Oliver, F. J. (2019). VE-cadherin promotes vasculogenic mimicry by
1167 modulating kaiso-dependent gene expression. Cell Death Differ *26*, 348-361.
1168 Demou, Z. N., and Hendrix, M. J. (2008). Microgenomics profile the endogenous angiogenic
1169 phenotype in subpopulations of aggressive melanoma. J Cell Biochem *105*, 562-573.
1170 Denko, N. C. (2008). Hypoxia, HIF1 and glucose metabolism in the solid tumour. Nat Rev
1171 Cancer *8*, 705-713.

1172 Du, J., Sun, B., Zhao, X., Gu, Q., Dong, X., Mo, J., Sun, T., Wang, J., Sun, R., and Liu, Y. (2014).
1173 Hypoxia promotes vasculogenic mimicry formation by inducing epithelial-mesenchymal
1174 transition in ovarian carcinoma. Gynecol Oncol *133*, 575-583.
1175 Duluc, D., Corvaisier, M., Blanchard, S., Catala, L., Descamps, P., Gamelin, E., Ponsoda, S.,
1176 Delneste, Y., Hebbar, M., and Jeannin, P. (2009). Interferon-gamma reverses the
1177 immunosuppressive and protumoral properties and prevents the generation of human tumor-
1178 associated macrophages. Int J Cancer *125*, 367-373.
1179 Duxbury, M. S., Ito, H., Zinner, M. J., Ashley, S. W., and Whang, E. E. (2004). EphA2: a
1180 determinant of malignant cellular behavior and a potential therapeutic target in pancreatic
1181 adenocarcinoma. Oncogene *23*, 1448-1456.
1182 Easty, D. J., Guthrie, B. A., Maung, K., Farr, C. J., Lindberg, R. A., Toso, R. J., Herlyn, M., and
1183 Bennett, D. C. (1995). Protein B61 as a new growth factor: expression of B61 and up-regulation
1184 of its receptor epithelial cell kinase during melanoma progression. Cancer Res *55*, 2528-2532.
1185 Eelen, G., de Zeeuw, P., Treps, L., Harjes, U., Wong, B. W., and Carmeliet, P. (2018). Endothelial
1186 Cell Metabolism. Physiol Rev *98*, 3-58.
1187 El Hallani, S., Boisselier, B., Peglion, F., Rousseau, A., Colin, C., Idbaih, A., Marie, Y., Mokhtari,
1188 K., Thomas, J. L., Eichmann, A.*, et al.* (2010). A new alternative mechanism in glioblastoma
1189 vascularization: tubular vasculogenic mimicry. Brain *133*, 973-982.
1190 Fan, M. J., Liang, S. M., He, P. J., Zhao, X. B., Li, M. J., and Geng, F. (2019). Dusp6 inhibits
1191 epithelial-mesenchymal transition in endometrial adenocarcinoma via ERK signaling pathway.
1192 Radiol Oncol *53*, 307-315.
1193 Folberg, R., and Maniotis, A. J. (2004). Vasculogenic mimicry. APMIS *112*, 508-525.
1194 Folkman, J. (1971). Tumor angiogenesis: therapeutic implications. N Engl J Med *285*, 1182-
1195 1186.
1196 Folkman, J. (1990). What is the evidence that tumors are angiogenesis dependent? J Natl
1197 Cancer Inst *82*, 4-6.
1198 Francescone, R., Scully, S., Bentley, B., Yan, W., Taylor, S. L., Oh, D., Moral, L., and Shao, R.
1199 (2012). Glioblastoma-derived tumor cells induce vasculogenic mimicry through Flk-1 protein
1200 activation. J Biol Chem *287*, 24821-24831.
1201 Frank, N. Y., Schatton, T., Kim, S., Zhan, Q., Wilson, B. J., Ma, J., Saab, K. R., Osherov, V.,
1202 Widlund, H. R., Gasser, M.*, et al.* (2011). VEGFR-1 expressed by malignant melanoma-initiating
1203 cells is required for tumor growth. Cancer Res *71*, 1474-1485.
1204 Gao, Y., Yu, H., Liu, Y., Liu, X., Zheng, J., Ma, J., Gong, W., Chen, J., Zhao, L., Tian, Y., and Xue,
1205 Y. (2018). Long Non-Coding RNA HOXA-AS2 Regulates Malignant Glioma Behaviors and
1206 Vasculogenic Mimicry Formation via the MiR-373/EGFR Axis. Cell Physiol Biochem *45*, 131-
1207 147.
1208 Gil, D., Ciołczyk-Wierzbicka, D., Dulińska-Litewka, J., and Laidler, P. (2016). Integrin-linked
1209 kinase regulates cadherin switch in bladder cancer. Tumour Biol *37*, 15185-15191.
1210 Gimbrone, M. A., Leapman, S. B., Cotran, R. S., and Folkman, J. (1972). Tumor dormancy in
1211 vivo by prevention of neovascularization. J Exp Med *136*, 261-276.
1212 Gong, W., Sun, B., Zhao, X., Zhang, D., Sun, J., Liu, T., Gu, Q., Dong, X., Liu, F., Wang, Y.*, et al.*
1213 (2016). Nodal signaling promotes vasculogenic mimicry formation in breast cancer via the
1214 Smad2/3 pathway. Oncotarget *7*, 70152-70167.
1215 Gorodetska, I., Lukiyanchuk, V., Peitzsch, C., Kozeretska, I., and Dubrovska, A. (2019). BRCA1
1216 and EZH2 cooperate in regulation of prostate cancer stem cell phenotype. Int J Cancer *145*,
1217 2974-2985.

1218 Graziani, G., Ruffini, F., Tentori, L., Scimeca, M., Dorio, A. S., Atzori, M. G., Failla, C. M., Morea,
1219 V., Bonanno, E., D'Atri, S., and Lacal, P. M. (2016). Antitumor activity of a novel anti-vascular
1220 endothelial growth factor receptor-1 monoclonal antibody that does not interfere with ligand
1221 binding. Oncotarget *7*, 72868-72885.
1222 Guo, J., Cai, H., Liu, X., Zheng, J., Liu, Y., Gong, W., Chen, J., Xi, Z., and Xue, Y. (2018). Long Non-
1223 coding RNA LINC00339 Stimulates Glioma Vasculogenic Mimicry Formation by Regulating the
1224 miR-539-5p/TWIST1/MMPs Axis. Mol Ther Nucleic Acids *10*, 170-186.
1225 Gupta, P. B., Onder, T. T., Jiang, G., Tao, K., Kuperwasser, C., Weinberg, R. A., and Lander, E. S.
1226 (2009). Identification of selective inhibitors of cancer stem cells by high-throughput screening.
1227 Cell *138*, 645-659.
1228 Hagemann, T., Lawrence, T., McNeish, I., Charles, K. A., Kulbe, H., Thompson, R. G., Robinson,
1229 S. C., and Balkwill, F. R. (2008). "Re-educating" tumor-associated macrophages by targeting
1230 NF-kappaB. J Exp Med *205*, 1261-1268.
1231 Hardy, K. M., Kirschmann, D. A., Seftor, E. A., Margaryan, N. V., Postovit, L. M., Strizzi, L., and
1232 Hendrix, M. J. (2010). Regulation of the embryonic morphogen Nodal by Notch4 facilitates
1233 manifestation of the aggressive melanoma phenotype. Cancer Res *70*, 10340-10350.
1234 Hendrix, M. J., Seftor, E. A., Meltzer, P. S., Gardner, L. M., Hess, A. R., Kirschmann, D. A.,
1235 Schatteman, G. C., and Seftor, R. E. (2001). Expression and functional significance of VE-
1236 cadherin in aggressive human melanoma cells: role in vasculogenic mimicry. Proc Natl Acad
1237 Sci U S A *98*, 8018-8023.
1238 Hess, A. R., Margaryan, N. V., Seftor, E. A., and Hendrix, M. J. (2007). Deciphering the signaling
1239 events that promote melanoma tumor cell vasculogenic mimicry and their link to embryonic
1240 vasculogenesis: role of the Eph receptors. Dev Dyn *236*, 3283-3296.
1241 Hess, A. R., Seftor, E. A., Gardner, L. M., Carles-Kinch, K., Schneider, G. B., Seftor, R. E., Kinch,
1242 M. S., and Hendrix, M. J. (2001). Molecular regulation of tumor cell vasculogenic mimicry by
1243 tyrosine phosphorylation: role of epithelial cell kinase (Eck/EphA2). Cancer Res *61*, 3250-3255.
1244 Hess, A. R., Seftor, E. A., Gruman, L. M., Kinch, M. S., Seftor, R. E., and Hendrix, M. J. (2006).
1245 VE-cadherin regulates EphA2 in aggressive melanoma cells through a novel signaling pathway:
1246 implications for vasculogenic mimicry. Cancer Biol Ther *5*, 228-233.
1247 Hong, H. N., Won, Y. J., Shim, J. H., Kim, H. J., Han, S. H., Kim, B. S., and Kim, H. S. (2018).
1248 Cancer-associated fibroblasts promote gastric tumorigenesis through EphA2 activation in a
1249 ligand-independent manner. J Cancer Res Clin Oncol *144*, 1649-1663.
1250 Hori, A., Shimoda, M., Naoi, Y., Kagara, N., Tanei, T., Miyake, T., Shimazu, K., Kim, S. J., and
1251 Noguchi, S. (2019). Vasculogenic mimicry is associated with trastuzumab resistance of HER2-
1252 positive breast cancer. Breast Cancer Res *21*, 88.
1253 Hsu, M. Y., Yang, M. H., Schnegg, C. I., Hwang, S., Ryu, B., and Alani, R. M. (2017). Notch3
1254 signaling-mediated melanoma-endothelial crosstalk regulates melanoma stem-like cell
1255 homeostasis and niche morphogenesis. Lab Invest *97*, 725-736.
1256 Hulin, J. A., Tommasi, S., Elliot, D., Hu, D. G., Lewis, B. C., and Mangoni, A. A. (2017). MiR-193b
1257 regulates breast cancer cell migration and vasculogenic mimicry by targeting dimethylarginine
1258 dimethylaminohydrolase 1. Sci Rep *7*, 13996.
1259 Hutchenreuther, J., Vincent, K., Norley, C., Racanelli, M., Gruber, S. B., Johnson, T. M., Fullen,
1260 D. R., Raskin, L., Perbal, B., Holdsworth, D. W.*, et al.* (2018). Activation of cancer-associated
1261 fibroblasts is required for tumor neovascularization in a murine model of melanoma. Matrix
1262 Biol *74*, 52-61.
1263 Islam, S. S., Mokhtari, R. B., Noman, A. S., Uddin, M., Rahman, M. Z., Azadi, M. A., Zlotta, A.,
1264 van der Kwast, T., Yeger, H., and Farhat, W. A. (2016). Sonic hedgehog (Shh) signaling

1265 promotes tumorigenicity and stemness via activation of epithelial-to-mesenchymal transition
1266 (EMT) in bladder cancer. Mol Carcinog *55*, 537-551.
1267 Izawa, Y., Kashii-Magaribuchi, K., Yoshida, K., Nosaka, M., Tsuji, N., Yamamoto, A., Kuroyanagi,
1268 K., Tono, K., Tanihata, M., Imanishi, M.*, et al.* (2018). Stem-like Human Breast Cancer Cells
1269 Initiate Vasculogenic Mimicry on Matrigel. Acta Histochem Cytochem *51*, 173-183.
1270 Jing, F., Ruan, X., Liu, X., Yang, C., Wang, D., Zheng, J., Xue, Y., Shen, S., Shao, L., Yang, Y.*, et al.*
1271 (2020). The PABPC5/HCG15/ZNF331 Feedback Loop Regulates Vasculogenic Mimicry of
1272 Glioma via STAU1-Mediated mRNA Decay. Mol Ther Oncolytics *17*, 216-231.
1273 Ju, R. J., Li, X. T., Shi, J. F., Li, X. Y., Sun, M. G., Zeng, F., Zhou, J., Liu, L., Zhang, C. X., Zhao, W.
1274 Y., and Lu, W. L. (2014). Liposomes, modified with PTD(HIV-1) peptide, containing epirubicin
1275 and celecoxib, to target vasculogenic mimicry channels in invasive breast cancer. Biomaterials
1276 *35*, 7610-7621.
1277 Kania, A., and Klein, R. (2016). Mechanisms of ephrin-Eph signalling in development,
1278 physiology and disease. Nat Rev Mol Cell Biol *17*, 240-256.
1279 Karagianni, P., and Wong, J. (2007). HDAC3: taking the SMRT-N-CoRrect road to repression.
1280 Oncogene *26*, 5439-5449.
1281 Kessenbrock, K., Plaks, V., and Werb, Z. (2010). Matrix metalloproteinases: regulators of the
1282 tumor microenvironment. Cell *141*, 52-67.
1283 Kim, H., Lee, S., Shin, E., Seong, K. M., Jin, Y. W., Youn, H., and Youn, B. (2020). The Emerging
1284 Roles of Exosomes as EMT Regulators in Cancer. Cells *9*.
1285 Kim, H. S., Won, Y. J., Shim, J. H., Kim, H. J., Kim, B. S., and Hong, H. N. (2019a). Role of EphA2-
1286 PI3K signaling in vasculogenic mimicry induced by cancer-associated fibroblasts in gastric
1287 cancer cells. Oncol Lett *18*, 3031-3038.
1288 Kim, H. S., Won, Y. J., Shim, J. H., Kim, H. J., Kim, J., Hong, H. N., and Kim, B. S. (2019b).
1289 Morphological characteristics of vasculogenic mimicry and its correlation with EphA2
1290 expression in gastric adenocarcinoma. Sci Rep *9*, 3414.
1291 Kim, K. J., Li, B., Winer, J., Armanini, M., Gillett, N., Phillips, H. S., and Ferrara, N. (1993).
1292 Inhibition of vascular endothelial growth factor-induced angiogenesis suppresses tumour
1293 growth in vivo. Nature *362*, 841-844.
1294 Ko, H., Jeon, H., Lee, D., Choi, H. K., Kang, K. S., and Choi, K. C. (2015). Sanguiin H6 suppresses
1295 TGF-β induction of the epithelial-mesenchymal transition and inhibits migration and invasion
1296 in A549 lung cancer. Bioorg Med Chem Lett *25*, 5508-5513.
1297 Kuczynski, E. A., Vermeulen, P. B., Pezzella, F., Kerbel, R. S., and Reynolds, A. R. (2019). Vessel
1298 co-option in cancer. Nat Rev Clin Oncol *16*, 469-493.
1299 Lapidot, T., Sirard, C., Vormoor, J., Murdoch, B., Hoang, T., Caceres-Cortes, J., Minden, M.,
1300 Paterson, B., Caligiuri, M. A., and Dick, J. E. (1994). A cell initiating human acute myeloid
1301 leukaemia after transplantation into SCID mice. Nature *367*, 645-648.
1302 Lathia, J. D., Mack, S. C., Mulkearns-Hubert, E. E., Valentim, C. L., and Rich, J. N. (2015). Cancer
1303 stem cells in glioblastoma. Genes Dev *29*, 1203-1217.
1304 Lenos, K. J., Miedema, D. M., Lodestijn, S. C., Nijman, L. E., van den Bosch, T., Romero Ros, X.,
1305 Lourenço, F. C., Lecca, M. C., van der Heijden, M., van Neerven, S. M.*, et al.* (2018). Stem cell
1306 functionality is microenvironmentally defined during tumour expansion and therapy response
1307 in colon cancer. Nat Cell Biol *20*, 1193-1202.
1308 Leskela, S., Pérez-Mies, B., Rosa-Rosa, J. M., Cristobal, E., Biscuola, M., Palacios-Berraquero,
1309 M. L., Ong, S., Matias-Guiu Guia, X., and Palacios, J. (2019). Molecular Basis of Tumor
1310 Heterogeneity in Endometrial Carcinosarcoma. Cancers (Basel) *11*.

1311 Li, C., Chen, Y., Zhang, Q., Guo, C., Chen, F., Xi, S., Zeng, J., Ke, C., Sharma, H. S., and Chen, Z.
1312 (2020). Expression of Twist associated to microcirculation patterns of human glioma
1313 correlated with progression and survival of the patient. Int Rev Neurobiol *151*, 201-217.
1314 Li, G., Huang, M., Cai, Y., Ke, Y., Yang, Y., and Sun, X. (2018a). miR-141 inhibits glioma
1315 vasculogenic mimicry by controlling EphA2 expression. Mol Med Rep *18*, 1395-1404.
1316 Li, S., and Wang, X. P. (2017). In vitro and in vivo evaluation of novel NGR-modified liposomes
1317 containing brucine. Int J Nanomedicine *12*, 5797-5804.
1318 Li, T., Zhang, C., Hassan, S., Liu, X., Song, F., Chen, K., Zhang, W., and Yang, J. (2018b). Histone
1319 deacetylase 6 in cancer. J Hematol Oncol *11*, 111.
1320 Li, X., Xue, Y., Liu, X., Zheng, J., Shen, S., Yang, C., Chen, J., Li, Z., Liu, L., Ma, J.*, et al.* (2019).
1321 ZRANB2/SNHG20/FOXK1 Axis regulates Vasculogenic mimicry formation in glioma. J Exp Clin
1322 Cancer Res *38*, 68.
1323 Li, Y., Sun, B., Zhao, X., Wang, X., Zhang, D., Gu, Q., and Liu, T. (2017a). MMP-2 and MMP-13
1324 affect vasculogenic mimicry formation in large cell lung cancer. J Cell Mol Med *21*, 3741-3751.
1325 Li, Y., Wu, Z., Yuan, J., Sun, L., Lin, L., Huang, N., Bin, J., Liao, Y., and Liao, W. (2017b). Long non-
1326 coding RNA MALAT1 promotes gastric cancer tumorigenicity and metastasis by regulating
1327 vasculogenic mimicry and angiogenesis. Cancer Lett *395*, 31-44.
1328 Liang, W., Song, S., Xu, Y., Li, H., and Liu, H. (2018). Knockdown of ZEB1 suppressed the
1329 formation of vasculogenic mimicry and epithelial-mesenchymal transition in the human breast
1330 cancer cell line MDA-MB-231. Mol Med Rep *17*, 6711-6716.
1331 Liang, X., Sun, R., Zhao, X., Zhang, Y., Gu, Q., Dong, X., Zhang, D., Sun, J., and Sun, B. (2017).
1332 Rictor regulates the vasculogenic mimicry of melanoma via the AKT-MMP-2/9 pathway. J Cell
1333 Mol Med *21*, 3579-3591.
1334 Liang, Y. J., Wang, Q. Y., Zhou, C. X., Yin, Q. Q., He, M., Yu, X. T., Cao, D. X., Chen, G. Q., He, J.
1335 R., and Zhao, Q. (2013). MiR-124 targets Slug to regulate epithelial-mesenchymal transition
1336 and metastasis of breast cancer. Carcinogenesis *34*, 713-722.
1337 Liew, F. Y., Girard, J. P., and Turnquist, H. R. (2016). Interleukin-33 in health and disease. Nat
1338 Rev Immunol *16*, 676-689.
1339 Ling, G., Ji, Q., Ye, W., Ma, D., and Wang, Y. (2016). Epithelial-mesenchymal transition
1340 regulated by p38/MAPK signaling pathways participates in vasculogenic mimicry formation in
1341 SHG44 cells transfected with TGF-β cDNA loaded lentivirus in vitro and in vivo. Int J Oncol *49*,
1342 2387-2398.
1343 Liou, G. Y. (2019). CD133 as a regulator of cancer metastasis through the cancer stem cells. Int
1344 J Biochem Cell Biol *106*, 1-7.
1345 Liu, R., Yang, K., Meng, C., Zhang, Z., and Xu, Y. (2012). Vasculogenic mimicry is a marker of
1346 poor prognosis in prostate cancer. Cancer Biol Ther *13*, 527-533.
1347 Liu, T., Zhang, Q., Zhang, J., Li, C., Miao, Y. R., Lei, Q., Li, Q., and Guo, A. Y. (2019). EVmiRNA: a
1348 database of miRNA profiling in extracellular vesicles. Nucleic Acids Res *47*, D89-D93.
1349 Liu, T. J., Guo, J. L., Wang, H. K., and Xu, X. (2018). Semaphorin-7A contributes to growth,
1350 migration and invasion of oral tongue squamous cell carcinoma through TGF-β-mediated EMT
1351 signaling pathway. Eur Rev Med Pharmacol Sci *22*, 1035-1043.
1352 Liu, W., Lv, C., Zhang, B., Zhou, Q., and Cao, Z. (2017). MicroRNA-27b functions as a new
1353 inhibitor of ovarian cancer-mediated vasculogenic mimicry through suppression of. RNA *23*,
1354 1019-1027.
1355 Liu, X., Wang, J. H., Li, S., Li, L. L., Huang, M., Zhang, Y. H., Liu, Y., Yang, Y. T., Ding, R., and Ke,
1356 Y. Q. (2015). Histone deacetylase 3 expression correlates with vasculogenic mimicry through

the phosphoinositide3-kinase / ERK-MMP-laminin5γ2 signaling pathway. Cancer Sci *106*, 857-866.

Liu, X. M., Zhang, Q. P., Mu, Y. G., Zhang, X. H., Sai, K., Pang, J. C., Ng, H. K., and Chen, Z. P. (2011a). Clinical significance of vasculogenic mimicry in human gliomas. Journal of neuro-oncology *105*, 173-179.

Liu, Z., Li, Y., Zhao, W., Ma, Y., and Yang, X. (2011b). Demonstration of vasculogenic mimicry in astrocytomas and effects of Endostar on U251 cells. Pathology, research and practice *207*, 645-651.

Lozano-Romero, A., Astudillo-de la Vega, H., Terrones-Gurrola, M. C. D. R., Marchat, L. A., Hernández-Sotelo, D., Salinas-Vera, Y. M., Ramos-Payan, R., Silva-Cázares, M. B., Nuñez-Olvera, S. I., Hernández-de la Cruz, O. N., and López-Camarillo, C. (2020). HOX Transcript Antisense RNA. Noncoding RNA *6*.

Lu, J., Lin, Y., Li, F., Ye, H., Zhou, R., Jin, Y., Li, B., Xiong, X., and Cheng, N. (2018). MiR-205 suppresses tumor growth, invasion, and epithelial-mesenchymal transition by targeting SEMA4C in hepatocellular carcinoma. FASEB J, fj201800113R.

Ma, J. L., Han, S. X., Zhu, Q., Zhao, J., Zhang, D., Wang, L., and Lv, Y. (2011). Role of Twist in vasculogenic mimicry formation in hypoxic hepatocellular carcinoma cells in vitro. Biochem Biophys Res Commun *408*, 686-691.

Ma, Y., Zhang, H., Xiong, C., Liu, Z., Xu, Q., Feng, J., Zhang, J., Wang, Z., and Yan, X. (2018). CD146 mediates an E-cadherin-to-N-cadherin switch during TGF-β signaling-induced epithelial-mesenchymal transition. Cancer Lett *430*, 201-214.

Maiti, A., Qi, Q., Peng, X., Yan, L., Takabe, K., and Hait, N. C. (2019). Class I histone deacetylase inhibitor suppresses vasculogenic mimicry by enhancing the expression of tumor suppressor and anti-angiogenesis genes in aggressive human TNBC cells. Int J Oncol *55*, 116-130.

Maniotis, A. J., Folberg, R., Hess, A., Seftor, E. A., Gardner, L. M., Pe'er, J., Trent, J. M., Meltzer, P. S., and Hendrix, M. J. (1999). Vascular channel formation by human melanoma cells in vivo and in vitro: vasculogenic mimicry. Am J Pathol *155*, 739-752.

Mao, Y., Zhu, L., Huang, Z., Luo, C., Zhou, T., Li, L., Wang, G., Yang, Z., Qi, W., Yang, X., and Gao, G. (2020). Stem-like tumor cells involved in heterogeneous vasculogenesis in breast cancer. Endocr Relat Cancer *27*, 23-39.

Massi, D., Tarantini, F., Franchi, A., Paglierani, M., Di Serio, C., Pellerito, S., Leoncini, G., Cirino, G., Geppetti, P., and Santucci, M. (2006). Evidence for differential expression of Notch receptors and their ligands in melanocytic nevi and cutaneous malignant melanoma. Mod Pathol *19*, 246-254.

McDonald, D. M., Munn, L., and Jain, R. K. (2000). Vasculogenic mimicry: how convincing, how novel, and how significant? Am J Pathol *156*, 383-388.

Mei, X., Chen, Y. S., Chen, F. R., Xi, S. Y., and Chen, Z. P. (2017). Glioblastoma stem cell differentiation into endothelial cells evidenced through live-cell imaging. Neuro Oncol *19*, 1109-1118.

Meng, J., Sun, B., Zhao, X., Zhang, D., Gu, Q., Dong, X., Zhao, N., Liu, P., and Liu, Y. (2014). Doxycycline as an inhibitor of the epithelial-to-mesenchymal transition and vasculogenic mimicry in hepatocellular carcinoma. Mol Cancer Ther *13*, 3107-3122.

Miro, C., Di Cicco, E., Ambrosio, R., Mancino, G., Di Girolamo, D., Cicatiello, A. G., Sagliocchi, S., Nappi, A., De Stefano, M. A., Luongo, C.*, et al.* (2019). Thyroid hormone induces progression and invasiveness of squamous cell carcinomas by promoting a ZEB-1/E-cadherin switch. Nat Commun *10*, 5410.

1403 Nakamura, R., Kataoka, H., Sato, N., Kanamori, M., Ihara, M., Igarashi, H., Ravshanov, S., Wang,
1404 Y. J., Li, Z. Y., Shimamura, T.*, et al.* (2005). EPHA2/EFNA1 expression in human gastric cancer.
1405 Cancer Sci *96*, 42-47.
1406 Nieto, M. A., Huang, R. Y., Jackson, R. A., and Thiery, J. P. (2016). EMT: 2016. Cell *166*, 21-45.
1407 Nievergall, E., Janes, P. W., Stegmayer, C., Vail, M. E., Haj, F. G., Teng, S. W., Neel, B. G.,
1408 Bastiaens, P. I., and Lackmann, M. (2010). PTP1B regulates Eph receptor function and
1409 trafficking. J Cell Biol *191*, 1189-1203.
1410 Orsenigo, F., Giampietro, C., Ferrari, A., Corada, M., Galaup, A., Sigismund, S., Ristagno, G.,
1411 Maddaluno, L., Koh, G. Y., Franco, D.*, et al.* (2012). Phosphorylation of VE-cadherin is
1412 modulated by haemodynamic forces and contributes to the regulation of vascular
1413 permeability in vivo. Nat Commun *3*, 1208.
1414 Pan, J. X., Wang, F., and Ye, L. Y. (2016). Doxorubicin-induced epithelial-mesenchymal
1415 transition through SEMA 4A in hepatocellular carcinoma. Biochem Biophys Res Commun *479*,
1416 610-614.
1417 Parri, M., Taddei, M. L., Bianchini, F., Calorini, L., and Chiarugi, P. (2009). EphA2 reexpression
1418 prompts invasion of melanoma cells shifting from mesenchymal to amoeboid-like motility
1419 style. Cancer Res *69*, 2072-2081.
1420 Pastorino, O., Gentile, M. T., Mancini, A., Del Gaudio, N., Di Costanzo, A., Bajetto, A., Franco,
1421 P., Altucci, L., Florio, T., Stoppelli, M. P., and Colucci-D'Amato, L. (2019). Histone Deacetylase
1422 Inhibitors Impair Vasculogenic Mimicry from Glioblastoma Cells. Cancers (Basel) *11*.
1423 Pastushenko, I., and Blanpain, C. (2019). EMT Transition States during Tumor Progression and
1424 Metastasis. Trends Cell Biol *29*, 212-226.
1425 Pautu, V., Mellinger, A., Resnier, P., Lepeltier, E., Martin, L., Boussemart, L., Letournel, F.,
1426 Passirani, C., and Clere, N. (2019). Melanoma tumour vasculature heterogeneity: from mice
1427 models to human. J Cancer Res Clin Oncol *145*, 589-597.
1428 Pavon, L. F., Sibov, T. T., de Souza, A. V., da Cruz, E. F., Malheiros, S. M. F., Cabral, F. R., de
1429 Souza, J. G., Boufleur, P., de Oliveira, D. M., de Toledo, S. R. C.*, et al.* (2018). Tropism of
1430 mesenchymal stem cell toward CD133. Stem Cell Res Ther *9*, 310.
1431 Peinado, H., Del Carmen Iglesias-de la Cruz, M., Olmeda, D., Csiszar, K., Fong, K. S., Vega, S.,
1432 Nieto, M. A., Cano, A., and Portillo, F. (2005). A molecular role for lysyl oxidase-like 2 enzyme
1433 in snail regulation and tumor progression. EMBO J *24*, 3446-3458.
1434 Peitzsch, C., Tyutyunnykova, A., Pantel, K., and Dubrovska, A. (2017). Cancer stem cells: The
1435 root of tumor recurrence and metastases. Semin Cancer Biol *44*, 10-24.
1436 Peng, Z., Wang, J., Shan, B., Li, B., Peng, W., Dong, Y., Shi, W., Zhao, W., He, D., Duan, M.*, et*
1437 *al.* (2018). The long noncoding RNA LINC00312 induces lung adenocarcinoma migration and
1438 vasculogenic mimicry through directly binding YBX1. Mol Cancer *17*, 167.
1439 Prieto-Vila, M., Yan, T., Calle, A. S., Nair, N., Hurley, L., Kasai, T., Kakuta, H., Masuda, J.,
1440 Murakami, H., Mizutani, A., and Seno, M. (2016). iPSC-derived cancer stem cells provide a
1441 model of tumor vasculature. Am J Cancer Res *6*, 1906-1921.
1442 Qi, L., Song, W., Liu, Z., Zhao, X., Cao, W., and Sun, B. (2015). Wnt3a Promotes the Vasculogenic
1443 Mimicry Formation of Colon Cancer via Wnt/β-Catenin Signaling. Int J Mol Sci *16*, 18564-
1444 18579.
1445 Qian, B. Z., and Pollard, J. W. (2010). Macrophage diversity enhances tumor progression and
1446 metastasis. Cell *141*, 39-51.
1447 Qin, Y., Zhao, W., Cheng, L., Wu, S., Wu, Q., Gao, J., Bian, Z., and Ma, L. (2019). Clinical
1448 significance of vasculogenic mimicry, vascular endothelial cadherin and SOX4 in patients with
1449 esophageal squamous cell carcinoma. Int J Clin Exp Pathol *12*, 2462-2473.

1450 Rai, A., and Cross, J. C. (2014). Development of the hemochorial maternal vascular spaces in
1451 the placenta through endothelial and vasculogenic mimicry. Dev Biol *387*, 131-141.
1452 Ren, D., Zhu, X., Kong, R., Zhao, Z., Sheng, J., Wang, J., Xu, X., Liu, J., Cui, K., Zhang, X. H.*, et al.*
1453 (2018). Targeting Brain-Adaptive Cancer Stem Cells Prohibits Brain Metastatic Colonization of
1454 Triple-Negative Breast Cancer. Cancer Res *78*, 2052-2064.
1455 Ribatti, D., Tamma, R., and Annese, T. (2020). Epithelial-Mesenchymal Transition in Cancer: A
1456 Historical Overview. Transl Oncol *13*, 100773.
1457 Ricci-Vitiani, L., Pallini, R., Biffoni, M., Todaro, M., Invernici, G., Cenci, T., Maira, G., Parati, E.
1458 A., Stassi, G., Larocca, L. M., and De Maria, R. (2010). Tumour vascularization via endothelial
1459 differentiation of glioblastoma stem-like cells. Nature *468*, 824-828.
1460 Robertson, F. M., Simeone, A. M., Lucci, A., McMurray, J. S., Ghosh, S., and Cristofanilli, M.
1461 (2010). Differential regulation of the aggressive phenotype of inflammatory breast cancer cells
1462 by prostanoid receptors EP3 and EP4. Cancer *116*, 2806-2814.
1463 Rong, X., Huang, B., Qiu, S., Li, X., He, L., and Peng, Y. (2016). Tumor-associated macrophages
1464 induce vasculogenic mimicry of glioblastoma multiforme through cyclooxygenase-2
1465 activation. Oncotarget *7*, 83976-83986.
1466 Ruf, W., Seftor, E. A., Petrovan, R. J., Weiss, R. M., Gruman, L. M., Margaryan, N. V., Seftor, R.
1467 E., Miyagi, Y., and Hendrix, M. J. (2003). Differential role of tissue factor pathway inhibitors 1
1468 and 2 in melanoma vasculogenic mimicry. Cancer Res *63*, 5381-5389.
1469 Sabet, O., Stockert, R., Xouri, G., Brüggemann, Y., Stanoev, A., and Bastiaens, P. I. H. (2015).
1470 Ubiquitination switches EphA2 vesicular traffic from a continuous safeguard to a finite
1471 signalling mode. Nat Commun *6*, 8047.
1472 Salinas-Vera, Y. M., Gallardo-Rincón, D., García-Vázquez, R., Hernández-de la Cruz, O. N.,
1473 Marchat, L. A., González-Barrios, J. A., Ruíz-García, E., Vázquez-Calzada, C., Contreras-Sanzón,
1474 E., Resendiz-Hernández, M.*, et al.* (2019). HypoxamiRs Profiling Identify miR-745 as a
1475 Regulator of the Early Stages of Vasculogenic Mimicry in SKOV3 Ovarian Cancer Cells. Front
1476 Oncol *9*, 381.
1477 Salinas-Vera, Y. M., Marchat, L. A., García-Vázquez, R., González de la Rosa, C. H., Castañeda-
1478 Saucedo, E., Tito, N. N., Flores, C. P., Pérez-Plasencia, C., Cruz-Colin, J. L., Carlos-Reyes, Á.*, et*
1479 *al.* (2018). Cooperative multi-targeting of signaling networks by angiomiR-204 inhibits
1480 vasculogenic mimicry in breast cancer cells. Cancer Lett *432*, 17-27.
1481 Sannino, G., Marchetto, A., Kirchner, T., and Grünewald, T. G. P. (2017). Epithelial-to-
1482 Mesenchymal and Mesenchymal-to-Epithelial Transition in Mesenchymal Tumors: A Paradox
1483 in Sarcomas? Cancer Res *77*, 4556-4561.
1484 Saxena, S., Purohit, A., Varney, M. L., Hayashi, Y., and Singh, R. K. (2018). Semaphorin-5A
1485 maintains epithelial phenotype of malignant pancreatic cancer cells. BMC Cancer *18*, 1283.
1486 Schatton, T., Murphy, G. F., Frank, N. Y., Yamaura, K., Waaga-Gasser, A. M., Gasser, M., Zhan,
1487 Q., Jordan, S., Duncan, L. M., Weishaupt, C.*, et al.* (2008). Identification of cells initiating
1488 human melanomas. Nature *451*, 345-349.
1489 Schnegg, C. I., Yang, M. H., Ghosh, S. K., and Hsu, M. Y. (2015). Induction of Vasculogenic
1490 Mimicry Overrides VEGF-A Silencing and Enriches Stem-like Cancer Cells in Melanoma. Cancer
1491 Res *75*, 1682-1690.
1492 Scully, S., Francescone, R., Faibish, M., Bentley, B., Taylor, S. L., Oh, D., Schapiro, R., Moral, L.,
1493 Yan, W., and Shao, R. (2012). Transdifferentiation of glioblastoma stem-like cells into mural
1494 cells drives vasculogenic mimicry in glioblastomas. J Neurosci *32*, 12950-12960.
1495 Seftor, E. A., Meltzer, P. S., Schatteman, G. C., Gruman, L. M., Hess, A. R., Kirschmann, D. A.,
1496 Seftor, R. E., and Hendrix, M. J. (2002). Expression of multiple molecular phenotypes by

aggressive melanoma tumor cells: role in vasculogenic mimicry. Crit Rev Oncol Hematol *44*, 17-27.

Seftor, R. E., Seftor, E. A., Koshikawa, N., Meltzer, P. S., Gardner, L. M., Bilban, M., Stetler-Stevenson, W. G., Quaranta, V., and Hendrix, M. J. (2001). Cooperative interactions of laminin 5 gamma2 chain, matrix metalloproteinase-2, and membrane type-1-matrix/metalloproteinase are required for mimicry of embryonic vasculogenesis by aggressive melanoma. Cancer Res *61*, 6322-6327.

Shao, B., Zhao, X., Liu, T., Zhang, Y., Sun, R., Dong, X., Liu, F., Zhao, N., Zhang, D., Wu, L.*, et al.* (2019). LOXL2 promotes vasculogenic mimicry and tumour aggressiveness in hepatocellular carcinoma. J Cell Mol Med *23*, 1363-1374.

Shetti, D., Zhang, B., Fan, C., Mo, C., Lee, B. H., and Wei, K. (2019). Low Dose of Paclitaxel Combined with XAV939 Attenuates Metastasis, Angiogenesis and Growth in Breast Cancer by Suppressing Wnt Signaling. Cells *8*.

Shih, I. M. (2011). Trophoblastic vasculogenic mimicry in gestational choriocarcinoma. Mod Pathol *24*, 646-652.

Shuai, Q., Cao, L., Qin, Z., Zhang, Y., Gu, Z., and Yang, J. (2020). VE-cadherin fusion protein substrate enhanced the vasculogenic mimicry capability of hepatocellular carcinoma cells. J Mater Chem B *8*, 1699-1712.

Song, J., and Li, Y. (2017). miR-25-3p reverses epithelial-mesenchymal transition via targeting Sema4C in cisplatin-resistance cervical cancer cells. Cancer Sci *108*, 23-31.

Song, Y., Mu, L., Han, X., Li, Q., Dong, B., Li, H., and Liu, X. (2013). MicroRNA-9 inhibits vasculogenic mimicry of glioma cell lines by suppressing Stathmin expression. J Neurooncol *115*, 381-390.

Sood, A. K., Seftor, E. A., Fletcher, M. S., Gardner, L. M., Heidger, P. M., Buller, R. E., Seftor, R. E., and Hendrix, M. J. (2001). Molecular determinants of ovarian cancer plasticity. Am J Pathol *158*, 1279-1288.

Spinella, F., Caprara, V., Di Castro, V., Rosanò, L., Cianfrocca, R., Natali, P. G., and Bagnato, A. (2013). Endothelin-1 induces the transactivation of vascular endothelial growth factor receptor-3 and modulates cell migration and vasculogenic mimicry in melanoma cells. J Mol Med (Berl) *91*, 395-405.

Su, S., Chen, J., Yao, H., Liu, J., Yu, S., Lao, L., Wang, M., Luo, M., Xing, Y., Chen, F.*, et al.* (2018). CD10. Cell *172*, 841-856.e816.

Sun, D., Sun, B., Liu, T., Zhao, X., Che, N., Gu, Q., Dong, X., Yao, Z., Li, R., Li, J.*, et al.* (2013). Slug promoted vasculogenic mimicry in hepatocellular carcinoma. J Cell Mol Med *17*, 1038-1047.

Sun, H., Yao, N., Cheng, S., Li, L., Liu, S., Yang, Z., Shang, G., Zhang, D., and Yao, Z. (2019). Cancer stem-like cells directly participate in vasculogenic mimicry channels in triple-negative breast cancer. Cancer Biol Med *16*, 299-311.

Sun, H., Zhang, D., Yao, Z., Lin, X., Liu, J., Gu, Q., Dong, X., Liu, F., Wang, Y., Yao, N.*, et al.* (2017). Anti-angiogenic treatment promotes triple-negative breast cancer invasion via vasculogenic mimicry. Cancer Biol Ther *18*, 205-213.

Sun, Q., Zou, X., Zhang, T., Shen, J., Yin, Y., and Xiang, J. (2014). The role of miR-200a in vasculogenic mimicry and its clinical significance in ovarian cancer. Gynecol Oncol *132*, 730-738.

Sun, T., Zhao, N., Zhao, X. L., Gu, Q., Zhang, S. W., Che, N., Wang, X. H., Du, J., Liu, Y. X., and Sun, B. C. (2010). Expression and functional significance of Twist1 in hepatocellular carcinoma: its role in vasculogenic mimicry. Hepatology *51*, 545-556.

1543 Sun, Y., Yue, S., Wang, Y., and Lu, F. (2018). Histone Deacetylase Inhibitors in Cancer Therapy.
1544 Curr Top Med Chem *18*, 2420-2428.
1545 Takasugi, M., Okada, R., Takahashi, A., Virya Chen, D., Watanabe, S., and Hara, E. (2017). Small
1546 extracellular vesicles secreted from senescent cells promote cancer cell proliferation through
1547 EphA2. Nat Commun *8*, 15729.
1548 Tam, K. J., Hui, D. H. F., Lee, W. W., Dong, M., Tombe, T., Jiao, I. Z. F., Khosravi, S., Takeuchi,
1549 A., Peacock, J. W., Ivanova, L.*, et al.* (2017). Semaphorin 3 C drives epithelial-to-mesenchymal
1550 transition, invasiveness, and stem-like characteristics in prostate cells. Sci Rep *7*, 11501.
1551 Tao, W., Sun, W., Zhu, H., and Zhang, J. (2018). Knockdown of long non-coding RNA TP73-AS1
1552 suppresses triple negative breast cancer cell vasculogenic mimicry by targeting miR-490-
1553 3p/TWIST1 axis. Biochem Biophys Res Commun *504*, 629-634.
1554 Thiery, J. P. (2002). Epithelial-mesenchymal transitions in tumour progression. Nat Rev Cancer
1555 *2*, 442-454.
1556 Thijssen, V. L., Paulis, Y. W., Nowak-Sliwinska, P., Deumelandt, K. L., Hosaka, K., Soetekouw, P.
1557 M., Cimpean, A. M., Raica, M., Pauwels, P., van den Oord, J. J.*, et al.* (2018). Targeting PDGF-
1558 mediated recruitment of pericytes blocks vascular mimicry and tumor growth. J Pathol *246*,
1559 447-458.
1560 Tkach, M., and Thery, C. (2016). Communication by Extracellular Vesicles: Where We Are and
1561 Where We Need to Go. Cell *164*, 1226-1232.
1562 Tomita, H., Tanaka, K., Tanaka, T., and Hara, A. (2016). Aldehyde dehydrogenase 1A1 in stem
1563 cells and cancer. Oncotarget *7*, 11018-11032.
1564 Topczewska, J. M., Postovit, L. M., Margaryan, N. V., Sam, A., Hess, A. R., Wheaton, W. W.,
1565 Nickoloff, B. J., Topczewski, J., and Hendrix, M. J. (2006). Embryonic and tumorigenic pathways
1566 converge via Nodal signaling: role in melanoma aggressiveness. Nat Med *12*, 925-932.
1567 Treps, L., Le Guelte, A., and Gavard, J. (2013). Emerging roles of Semaphorins in the regulation
1568 of epithelial and endothelial junctions. Tissue Barriers *1*, e23272.
1569 Tseng, C. H., Murray, K. D., Jou, M. F., Hsu, S. M., Cheng, H. J., and Huang, P. H. (2011).
1570 Sema3E/plexin-D1 mediated epithelial-to-mesenchymal transition in ovarian endometrioid
1571 cancer. PLoS One *6*, e19396.
1572 Valdivia, A., Mingo, G., Aldana, V., Pinto, M. P., Ramirez, M., Retamal, C., Gonzalez, A., Nualart,
1573 F., Corvalan, A. H., and Owen, G. I. (2019). Fact or Fiction, It Is Time for a Verdict on
1574 Vasculogenic Mimicry? Front Oncol *9*, 680.
1575 van der Schaft, D. W., Hillen, F., Pauwels, P., Kirschmann, D. A., Castermans, K., Egbrink, M. G.,
1576 Tran, M. G., Sciot, R., Hauben, E., Hogendoorn, P. C.*, et al.* (2005). Tumor cell plasticity in Ewing
1577 sarcoma, an alternative circulatory system stimulated by hypoxia. Cancer Res *65*, 11520-
1578 11528.
1579 Vartanian, A., Gatsina, G., Grigorieva, I., Solomko, E., Dombrovsky, V., Baryshnikov, A., and
1580 Stepanova, E. (2013). The involvement of Notch signaling in melanoma vasculogenic mimicry.
1581 Clin Exp Med *13*, 201-209.
1582 Vartanian, A., Stepanova, E., Grigorieva, I., Solomko, E., Baryshnikov, A., and Lichinitser, M.
1583 (2011). VEGFR1 and PKCα signaling control melanoma vasculogenic mimicry in a VEGFR2
1584 kinase-independent manner. Melanoma Res *21*, 91-98.
1585 Virant-Klun, I., Skerl, P., Novakovic, S., Vrtacnik-Bokal, E., and Smrkolj, S. (2019). Similar
1586 Population of CD133+ and DDX4+ VSEL-Like Stem Cells Sorted from Human Embryonic Stem
1587 Cell, Ovarian, and Ovarian Cancer Ascites Cell Cultures: The Real Embryonic Stem Cells? Cells
1588 *8*.

1589 Vishnubalaji, R., Manikandan, M., Fahad, M., Hamam, R., Alfayez, M., Kassem, M., Aldahmash,
1590 A., and Alajez, N. M. (2018). Molecular profiling of ALDH1. Oncotarget *9*, 13551-13564.
1591 Wagenblast, E., Soto, M., Gutiérrez-Ángel, S., Hartl, C. A., Gable, A. L., Maceli, A. R., Erard, N.,
1592 Williams, A. M., Kim, S. Y., Dickopf, S.*, et al.* (2015). A model of breast cancer heterogeneity
1593 reveals vascular mimicry as a driver of metastasis. Nature *520*, 358-362.
1594 Walker-Daniels, J., Riese, D. J., and Kinch, M. S. (2002). c-Cbl-dependent EphA2 protein
1595 degradation is induced by ligand binding. Mol Cancer Res *1*, 79-87.
1596 Wang, H., Sun, W., Zhang, W. Z., Ge, C. Y., Zhang, J. T., Liu, Z. Y., and Fan, Y. Z. (2014). Inhibition
1597 of tumor vasculogenic mimicry and prolongation of host survival in highly aggressive
1598 gallbladder cancers by norcantharidin via blocking the ephrin type a receptor 2/focal adhesion
1599 kinase/paxillin signaling pathway. PLoS One *9*, e96982.
1600 Wang, H. F., Wang, S. S., Zheng, M., Dai, L. L., Wang, K., Gao, X. L., Cao, M. X., Yu, X. H., Pang,
1601 X., Zhang, M.*, et al.* (2019). Hypoxia promotes vasculogenic mimicry formation by vascular
1602 endothelial growth factor A mediating epithelial-mesenchymal transition in salivary adenoid
1603 cystic carcinoma. Cell Prolif *52*, e12600.
1604 Wang, L., Song, Y., Wang, H., Liu, K., Shao, Z., and Shang, Z. (2020a). MiR-210-3p-EphrinA3-
1605 PI3K/AKT axis regulates the progression of oral cancer. J Cell Mol Med *24*, 4011-4022.
1606 Wang, M., Yang, C., Liu, X., Zheng, J., Xue, Y., Ruan, X., Shen, S., Wang, D., Li, Z., Cai, H., and
1607 Liu, Y. (2020b). An upstream open reading frame regulates vasculogenic mimicry of glioma via
1608 ZNRD1-AS1/miR-499a-5p/ELF1/EMI1 pathway. J Cell Mol Med.
1609 Wang, M., Zhao, X., Zhu, D., Liu, T., Liang, X., Liu, F., Zhang, Y., Dong, X., and Sun, B. (2017).
1610 HIF-1α promoted vasculogenic mimicry formation in hepatocellular carcinoma through LOXL2
1611 up-regulation in hypoxic tumor microenvironment. J Exp Clin Cancer Res *36*, 60.
1612 Wang, R., Chadalavada, K., Wilshire, J., Kowalik, U., Hovinga, K. E., Geber, A., Fligelman, B.,
1613 Leversha, M., Brennan, C., and Tabar, V. (2010). Glioblastoma stem-like cells give rise to
1614 tumour endothelium. Nature *468*, 829-833.
1615 Wang, S. Y., Ke, Y. Q., Lu, G. H., Song, Z. H., Yu, L., Xiao, S., Sun, X. L., Jiang, X. D., Yang, Z. L.,
1616 and Hu, C. C. (2013). Vasculogenic mimicry is a prognostic factor for postoperative survival in
1617 patients with glioblastoma. J Neurooncol *112*, 339-345.
1618 Wang, S. Y., Yu, L., Ling, G. Q., Xiao, S., Sun, X. L., Song, Z. H., Liu, Y. J., Jiang, X. D., Cai, Y. Q.,
1619 and Ke, Y. Q. (2012). Vasculogenic mimicry and its clinical significance in medulloblastoma.
1620 Cancer Biol Ther *13*, 341-348.
1621 Wang, Y., Yang, R., Wang, X., Ci, H., Zhou, L., Zhu, B., Wu, S., and Wang, D. (2018). Evaluation
1622 of the correlation of vasculogenic mimicry, Notch4, DLL4, and KAI1/CD82 in the prediction of
1623 metastasis and prognosis in non-small cell lung cancer. Medicine (Baltimore) *97*, e13817.
1624 Wang, Z., Chen, J., Zhang, W., Zheng, Y., Liu, L., Wu, H., Ye, J., Qi, B., Wu, Y., and Song, X. (2016).
1625 Axon guidance molecule semaphorin3A is a novel tumor suppressor in head and neck
1626 squamous cell carcinoma. Oncotarget *7*, 6048-6062.
1627 Wendt, M. K., Allington, T. M., and Schiemann, W. P. (2009). Mechanisms of the epithelial-
1628 mesenchymal transition by TGF-beta. Future oncology *5*, 1145-1168.
1629 Wheelock, M. J., Shintani, Y., Maeda, M., Fukumoto, Y., and Johnson, K. R. (2008). Cadherin
1630 switching. J Cell Sci *121*, 727-735.
1631 Wigerup, C., Påhlman, S., and Bexell, D. (2016). Therapeutic targeting of hypoxia and hypoxia-
1632 inducible factors in cancer. Pharmacol Ther *164*, 152-169.
1633 Williamson, S. C., Metcalf, R. L., Trapani, F., Mohan, S., Antonello, J., Abbott, B., Leong, H. S.,
1634 Chester, C. P., Simms, N., Polanski, R.*, et al.* (2016). Vasculogenic mimicry in small cell lung
1635 cancer. Nat Commun *7*, 13322.

1636 Wu, H. B., Yang, S., Weng, H. Y., Chen, Q., Zhao, X. L., Fu, W. J., Niu, Q., Ping, Y. F., Wang, J. M.,
1637 Zhang, X.*, et al.* (2017). Autophagy-induced KDR/VEGFR-2 activation promotes the formation
1638 of vasculogenic mimicry by glioma stem cells. Autophagy *13*, 1528-1542.
1639 Wu, N., Zhao, X., Liu, M., Liu, H., Yao, W., Zhang, Y., Cao, S., and Lin, X. (2011). Role of
1640 microRNA-26b in glioma development and its mediated regulation on EphA2. PLoS One *6*,
1641 e16264.
1642 Wurmser, A. E., Nakashima, K., Summers, R. G., Toni, N., D'Amour, K. A., Lie, D. C., and Gage,
1643 F. H. (2004). Cell fusion-independent differentiation of neural stem cells to the endothelial
1644 lineage. Nature *430*, 350-356.
1645 Xia, Y., Cai, X., Fan, J., Zhang, L., Li, Z., Ren, J., Wu, G., and Zhu, F. (2017). RhoA/ROCK pathway
1646 inhibition by fasudil suppresses the vasculogenic mimicry of U2OS osteosarcoma cells in vitro.
1647 Anticancer Drugs *28*, 514-521.
1648 Xia, Y., Cai, X. Y., Fan, J. Q., Zhang, L. L., Ren, J. H., Chen, J., Li, Z. Y., Zhang, R. G., Zhu, F., and
1649 Wu, G. (2015). Rho Kinase Inhibitor Fasudil Suppresses the Vasculogenic Mimicry of B16
1650 Mouse Melanoma Cells Both In Vitro and In Vivo. Mol Cancer Ther *14*, 1582-1590.
1651 Xia, Y., Cai, X. Y., Fan, J. Q., Zhang, L. L., Ren, J. H., Li, Z. Y., Zhang, R. G., Zhu, F., and Wu, G.
1652 (2019). The role of sema4D in vasculogenic mimicry formation in non-small cell lung cancer
1653 and the underlying mechanisms. Int J Cancer *144*, 2227-2238.
1654 Xiang, T., Lin, Y. X., Ma, W., Zhang, H. J., Chen, K. M., He, G. P., Zhang, X., Xu, M., Feng, Q. S.,
1655 Chen, M. Y.*, et al.* (2018). Vasculogenic mimicry formation in EBV-associated epithelial
1656 malignancies. Nat Commun *9*, 5009.
1657 Xiao, T., Zhong, W., Zhao, J., Qian, B., Liu, H., Chen, S., Qiao, K., Lei, Y., Zong, S., Wang, H.*, et*
1658 *al.* (2018). Polyphyllin I suppresses the formation of vasculogenic mimicry via Twist1/VE-
1659 cadherin pathway. Cell Death Dis *9*, 906.
1660 Xu, J., Zhang, Y., Wang, Y., Tao, X., Cheng, L., Wu, S., and Tao, Y. (2018a). Correlation of KAI1,
1661 CD133 and vasculogenic mimicry with the prediction of metastasis and prognosis in
1662 hepatocellular carcinoma. Int J Clin Exp Pathol *11*, 3638-3646.
1663 Xu, M. R., Wei, P. F., Suo, M. Z., Hu, Y., Ding, W., Su, L., Zhu, Y. D., Song, W. J., Tang, G. H.,
1664 Zhang, M., and Li, P. (2019). Brucine Suppresses Vasculogenic Mimicry in Human Triple-
1665 Negative Breast Cancer Cell Line MDA-MB-231. Biomed Res Int *2019*, 6543230.
1666 Xu, S., Bai, J., Zhuan, Z., Li, B., Zhang, Z., Wu, X., Luo, X., and Yang, L. (2018b). EBV-LMP1 is
1667 involved in vasculogenic mimicry formation via VEGFA/VEGFR1 signaling in nasopharyngeal
1668 carcinoma. Oncol Rep *40*, 377-384.
1669 Xu, S., Zhang, J., Xue, H., Guo, X., Han, X., Li, T., Gao, X., Liu, Q., and Li, G. (2017). MicroRNA-
1670 584-3p reduces the vasculogenic mimicry of human glioma cells by regulating hypoxia-induced
1671 ROCK1 dependent stress fiber formation. Neoplasma *64*, 13-21.
1672 Xue, H., Gao, X., Xu, S., Zhang, J., Guo, X., Yan, S., Li, T., Liu, Q., and Li, G. (2016). MicroRNA-
1673 Let-7f reduces the vasculogenic mimicry of human glioma cells by regulating periostin-
1674 dependent migration. Oncol Rep *35*, 1771-1777.
1675 Xue, Y., Sun, R., Zheng, W., Yang, L., and An, R. (2020). Forskolin promotes vasculogenic
1676 mimicry and invasion via Notch-1-activated epithelial-to-mesenchymal transition in
1677 syncytiolization of trophoblast cells in choriocarcinoma. Int J Oncol *56*, 1129-1139.
1678 Yang, F., Wen, M., Pan, D., Lin, X., Mo, J., Dong, X., Liao, S., and Ma, Y. (2019). IL-33/ST2 Axis
1679 Regulates Vasculogenic Mimicry via ERK1/2-MMP-2/9 Pathway in Melanoma. Dermatology
1680 *235*, 225-233.

Yang, J., Lu, Y., Lin, Y. Y., Zheng, Z. Y., Fang, J. H., He, S., and Zhuang, S. M. (2016). Vascular mimicry formation is promoted by paracrine TGF-β and SDF1 of cancer-associated fibroblasts and inhibited by miR-101 in hepatocellular carcinoma. Cancer Lett *383*, 18-27.

Yang, Q., Wang, Y., Lu, X., Zhao, Z., Zhu, L., Chen, S., Wu, Q., Chen, C., and Wang, Z. (2015a). MiR-125b regulates epithelial-mesenchymal transition via targeting Sema4C in paclitaxel-resistant breast cancer cells. Oncotarget *6*, 3268-3279.

Yang, S., Liu, Y., Li, M. Y., Ng, C. S. H., Yang, S. L., Wang, S., Zou, C., Dong, Y., Du, J., Long, X.*, et al.* (2017). FOXP3 promotes tumor growth and metastasis by activating Wnt/β-catenin signaling pathway and EMT in non-small cell lung cancer. Mol Cancer *16*, 124.

Yang, Y. H., Markus, M. A., Mangs, A. H., Raitskin, O., Sperling, R., and Morris, B. J. (2013). ZRANB2 localizes to supraspliceosomes and influences the alternative splicing of multiple genes in the transcriptome. Mol Biol Rep *40*, 5381-5395.

Yang, Z., Sun, B., Li, Y., Zhao, X., Gu, Q., An, J., Dong, X., Liu, F., and Wang, Y. (2015b). ZEB2 promotes vasculogenic mimicry by TGF-β1 induced epithelial-to-mesenchymal transition in hepatocellular carcinoma. Exp Mol Pathol *98*, 352-359.

Yao, N., Ren, K., Gu, X. J., Wu, S. J., Shi, X., Chang, Q., Li, Y. G., Gao, Z. X., Jin, Q. M., Zhang, J.*, et al.* (2020). Identification of potential crucial genes associated with vasculogenic mimicry in human osteosarcoma based on gene expression profile. Neoplasma *67*, 286-295.

Yao, X., Ping, Y., Liu, Y., Chen, K., Yoshimura, T., Liu, M., Gong, W., Chen, C., Niu, Q., Guo, D.*, et al.* (2013). Vascular endothelial growth factor receptor 2 (VEGFR-2) plays a key role in vasculogenic mimicry formation, neovascularization and tumor initiation by Glioma stem-like cells. PLoS One *8*, e57188.

Yin, A. H., Miraglia, S., Zanjani, E. D., Almeida-Porada, G., Ogawa, M., Leary, A. G., Olweus, J., Kearney, J., and Buck, D. W. (1997). AC133, a novel marker for human hematopoietic stem and progenitor cells. Blood *90*, 5002-5012.

Yu, W., Ding, J., He, M., Chen, Y., Wang, R., Han, Z., Xing, E. Z., Zhang, C., and Yeh, S. (2019). Estrogen receptor β promotes the vasculogenic mimicry (VM) and cell invasion via altering the lncRNA-MALAT1/miR-145-5p/NEDD9 signals in lung cancer. Oncogene *38*, 1225-1238.

Yue, W. Y., and Chen, Z. P. (2005). Does vasculogenic mimicry exist in astrocytoma? J Histochem Cytochem *53*, 997-1002.

Yue, Z., Yuan, Z., Zeng, L., Wang, Y., Lai, L., Li, J., Sun, P., Xue, X., Qi, J., Yang, Z.*, et al.* (2018). LGR4 modulates breast cancer initiation, metastasis, and cancer stem cells. FASEB J *32*, 2422-2437.

Zavros, Y. (2017). Initiation and Maintenance of Gastric Cancer: A Focus on CD44 Variant Isoforms and Cancer Stem Cells. Cell Mol Gastroenterol Hepatol *4*, 55-63.

Zhang, C., Chen, W., Zhang, X., Huang, B., Chen, A., He, Y., Wang, J., and Li, X. (2016). Galunisertib inhibits glioma vasculogenic mimicry formation induced by astrocytes. Sci Rep *6*, 23056.

Zhang, D., Sun, B., Zhao, X., Ma, Y., Ji, R., Gu, Q., Dong, X., Li, J., Liu, F., Jia, X.*, et al.* (2014a). Twist1 expression induced by sunitinib accelerates tumor cell vasculogenic mimicry by increasing the population of CD133+ cells in triple-negative breast cancer. Mol Cancer *13*, 207.

Zhang, D., Sun, B., Zhao, X., Sun, H., An, J., Lin, X., Zhu, D., Wang, X., Liu, F., Zhang, Y.*, et al.* (2020). Twist1 accelerates tumour vasculogenic mimicry by inhibiting Claudin15 expression in triple-negative breast cancer. J Cell Mol Med.

Zhang, J. G., Li, X. Y., Wang, Y. Z., Zhang, Q. D., Gu, S. Y., Wu, X., Zhu, G. H., Li, Q., and Liu, G. L. (2014b). ROCK is involved in vasculogenic mimicry formation in hepatocellular carcinoma cell line. PLoS One *9*, e107661.

1728 Zhang, J. G., Zhang, D. D., Wu, X., Wang, Y. Z., Gu, S. Y., Zhu, G. H., Li, X. Y., Li, Q., and Liu, G. L.
1729 (2015a). Incarvine C suppresses proliferation and vasculogenic mimicry of hepatocellular
1730 carcinoma cells via targeting ROCK inhibition. BMC Cancer *15*, 814.
1731 Zhang, L., Xu, Y., Sun, J., Chen, W., Zhao, L., Ma, C., Wang, Q., Huang, B., Zhang, Y., Li, X., and
1732 Qu, X. (2017). M2-like tumor-associated macrophages drive vasculogenic mimicry through
1733 amplification of IL-6 expression in glioma cells. Oncotarget *8*, 819-832.
1734 Zhang, S., Fu, Z., Wei, J., Guo, J., Liu, M., and Du, K. (2015b). Peroxiredoxin 2 is involved in
1735 vasculogenic mimicry formation by targeting VEGFR2 activation in colorectal cancer. Med
1736 Oncol *32*, 414.
1737 Zhang, S., Li, M., Zhang, D., Xu, S., Wang, X., Liu, Z., Zhao, X., and Sun, B. (2009). Hypoxia
1738 influences linearly patterned programmed cell necrosis and tumor blood supply patterns
1739 formation in melanoma. Lab Invest *89*, 575-586.
1740 Zhang, W., Zhou, P., Meng, A., Zhang, R., and Zhou, Y. (2018). Down-regulating Myoferlin
1741 inhibits the vasculogenic mimicry of melanoma via decreasing MMP-2 and inducing
1742 mesenchymal-to-epithelial transition. J Cell Mol Med *22*, 1743-1754.
1743 Zhao, N., Sun, H., Sun, B., Zhu, D., Zhao, X., Wang, Y., Gu, Q., Dong, X., Liu, F., Zhang, Y., and Li,
1744 X. (2016a). miR-27a-3p suppresses tumor metastasis and VM by down-regulating VE-cadherin
1745 expression and inhibiting EMT: an essential role for Twist-1 in HCC. Sci Rep *6*, 23091.
1746 Zhao, X., Sun, B., Li, Y., Liu, Y., Zhang, D., Wang, X., Gu, Q., Zhao, J., Dong, X., Liu, Z., and Che,
1747 N. (2015). Dual effects of collagenase-3 on melanoma: metastasis promotion and disruption
1748 of vasculogenic mimicry. Oncotarget *6*, 8890-8899.
1749 Zhao, X., Sun, B., Liu, T., Shao, B., Sun, R., Zhu, D., Zhang, Y., Gu, Q., Dong, X., Liu, F*., et al.*
1750 (2018). Long noncoding RNA n339260 promotes vasculogenic mimicry and cancer stem cell
1751 development in hepatocellular carcinoma. Cancer Sci *109*, 3197-3208.
1752 Zhao, X., Wang, Y., Deng, R., Zhang, H., Dou, J., Yuan, H., Hou, G., Du, Y., Chen, Q., and Yu, J.
1753 (2016b). miR186 suppresses prostate cancer progression by targeting Twist1. Oncotarget *7*,
1754 33136-33151.
1755 Zhao, Z., Xiang, S., Qi, J., Wei, Y., Zhang, M., Yao, J., Zhang, T., Meng, M., Wang, X., and Zhou,
1756 Q. (2020). Correction of the tumor suppressor Salvador homolog-1 deficiency in tumors by
1757 lycorine as a new strategy in lung cancer therapy. Cell Death Dis *11*, 387.
1758 Zhong, Z., Yu, J., Virshup, D. M., and Madan, B. (2020). Wnts and the hallmarks of cancer.
1759 Cancer Metastasis Rev.
1760 Zhou, J., Wang, H., Che, J., Xu, L., Yang, W., Li, Y., and Zhou, W. (2020). Silencing of microRNA-
1761 135b inhibits invasion, migration, and stemness of CD24. Cancer Cell Int *20*, 134.
1762 Zhuo, M., Yuan, C., Han, T., Hu, H., Cui, J., Jiao, F., and Wang, L. (2019). JQ1 effectively inhibits
1763 vasculogenic mimicry of pancreatic ductal adenocarcinoma cells via the ERK1/2-MMP-2/9
1764 signaling pathway both in vitro and in vivo. Am J Transl Res *11*, 1030-1039.
1765 Zigrino, P., Kuhn, I., Bäuerle, T., Zamek, J., Fox, J. W., Neumann, S., Licht, A., Schorpp-Kistner,
1766 M., Angel, P., and Mauch, C. (2009). Stromal expression of MMP-13 is required for melanoma
1767 invasion and metastasis. J Invest Dermatol *129*, 2686-2693.
1768

Figure 1

A Patterned vascular mimicry

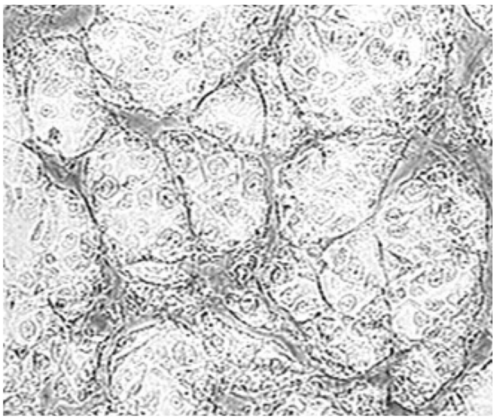

B Tubular vascular mimicry

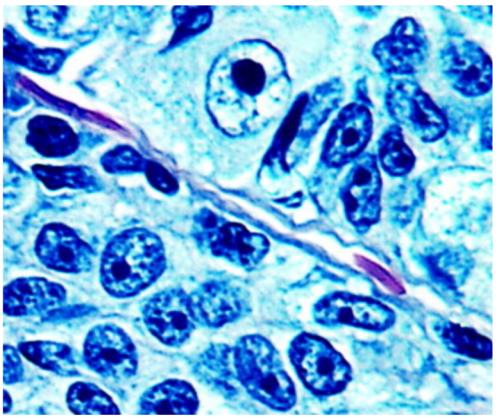

Figure 2

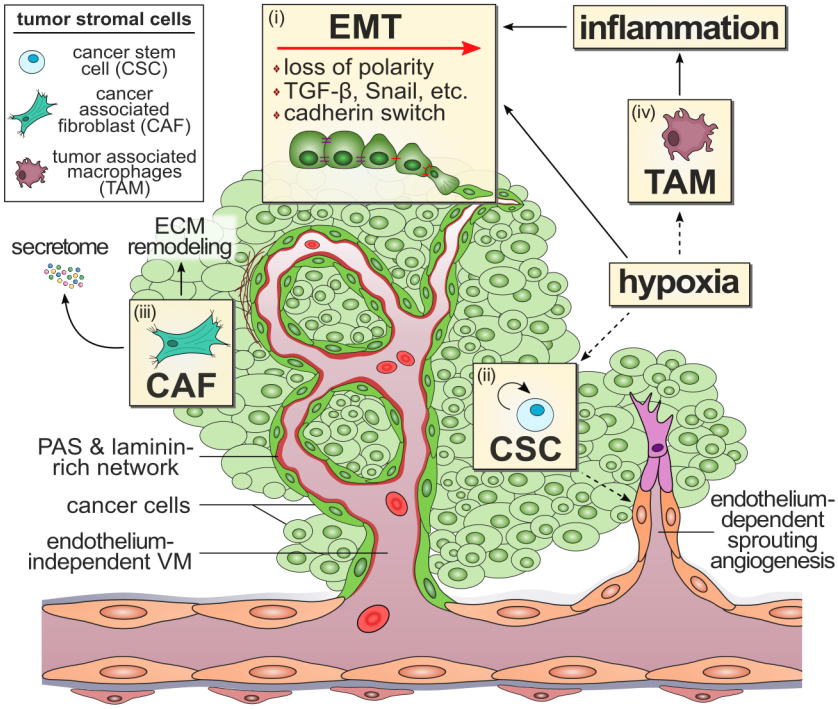
tumor stromal cells
cancer stem cell (CSC)
cancer associated fibroblast (CAF)
tumor associated macrophages (TAM)
(i)
EMT
loss of polarity
TGF-β, Snail, etc.
cadherin switch
inflammation
(iv)
TAM
hypoxia
ECM remodeling
secretome
(iii)
CAF
(ii)
CSC
PAS & laminin-rich network
cancer cells
endothelium-independent VM
endothelium-dependent sprouting angiogenesis

Figure 3

A VEGF/VEGFR-related signaling

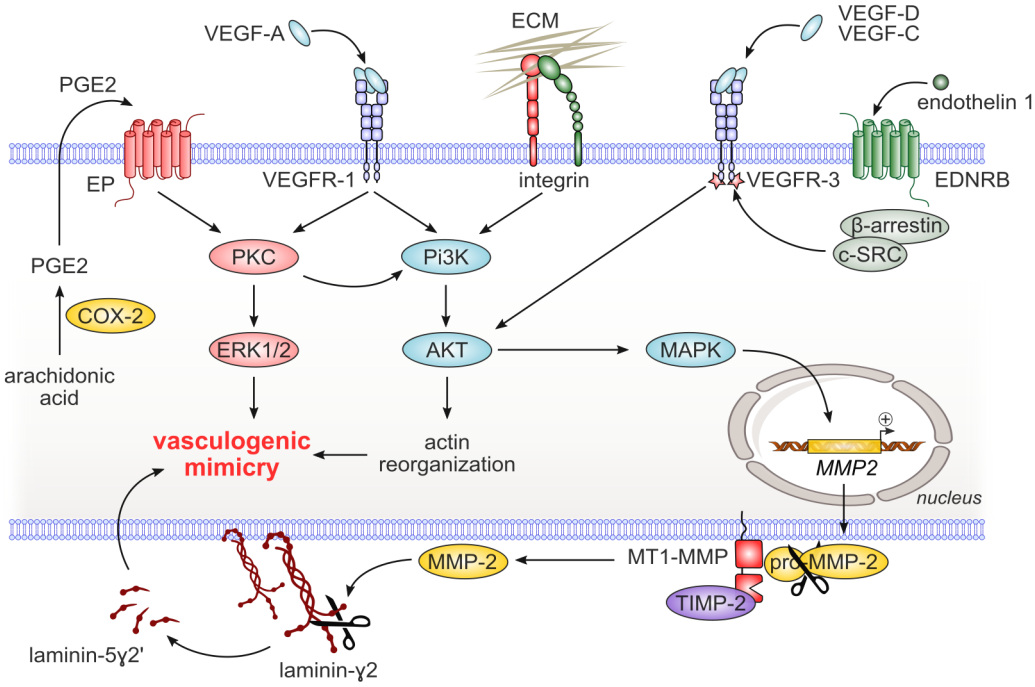

B VE-cadherin-related signaling

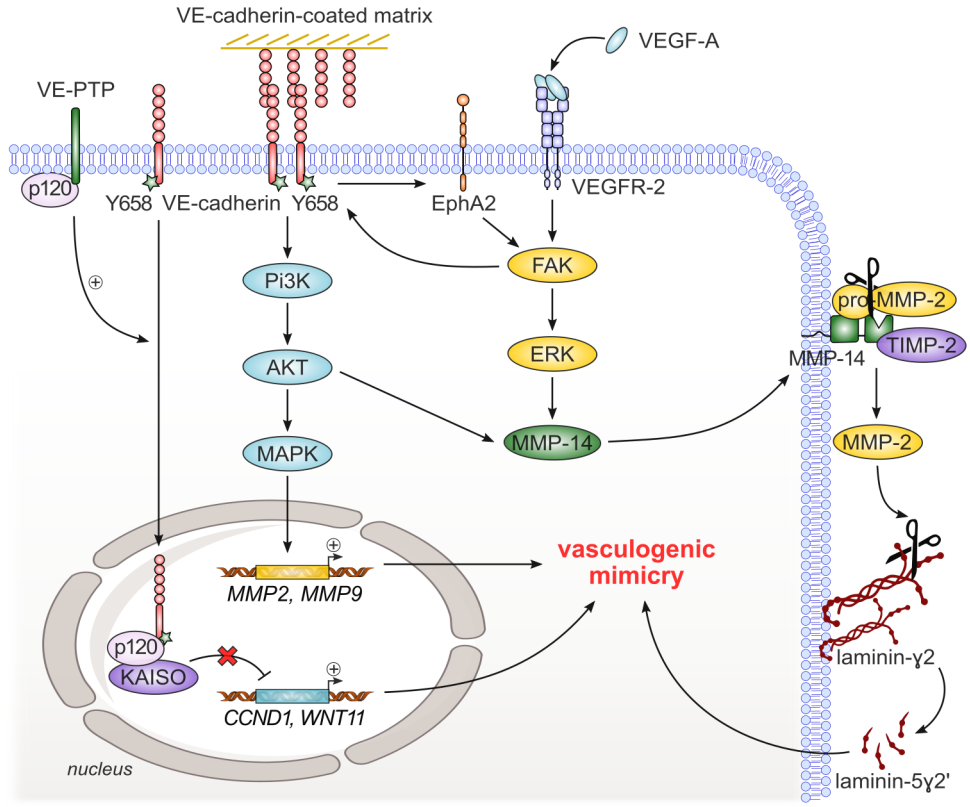

Table 1
Non-coding RNAs involved during vasculogenic mimicry.

ncRNAs	Cancer type	Signaling involved	miRNA involved	Effect on VM	References
miRNAs:					
miR-204	TNBC	PI3K/AKT, RAF1/MAPK, VEGF, and FAK/SRC signaling	n/a	suppress	(Salinas-Vera et al., 2018); (Lozano-Romero et al., 2020)
miR-490-3p	breast cancer; clear cell renal cell carcinoma	Twist1 and vimentin targeting	n/a	suppress	(Zhang, Li, et al., 2014b); (Tao et al., 2018)
miR-193b	breast cancer	DDAH1 targeting	n/a	suppress	(Hulin et al., 2017)
miR-124	breast cancer; cervical cancer	Slug targeting; interact with AmotL1 to reduce invasion and VM	n/a	suppress	(Liang et al., 2013)
miR-765	ovarian cancer	decrease VEGF-A and AKT/SRC signaling	n/a	suppress	(Salinas-Vera et al., 2019)
miR-200a	ovarian cancer	EphA2 targeting	n/a	suppress	(Sun et al., 2014)
miR-141	glioma				(Li, Huang, et al., 2018a)
miR-26b	glioma		n/a		(Wu et al., 2011)
			n/a		
miR-27b	ovarian cancer	VE-cadherin targeting	n/a	suppress	(Liu et al., 2017)
miR-27a-3p	HCC		n/a		(Zhao, Sun, et al., 2016a)
miR-450a-5p	colorectal cancer	suppress SOX2 expression	n/a	suppress	(Chen et al., 2020)
miR-101	HCC	target TGF-ßR1 and Smad2 in tumor cells, and reduce SDF1 levels in CAFs	n/a	suppress	(Yang et al., 2016)
miR-186	prostate cancer	Twist1 targeting	n/a	suppress	(Zhao et al., 2016b)
miR-Let-7f	glioma	periostin targeting	n/a	suppress	(Xue et al., 2016)
miR-9	glioma	stathmin 1 targeting	n/a	suppress	(Song et al., 2013)
miR-584-3p	glioma	ROCK1 targeting	n/a	suppress	(Xu et al., 2017)
LncRNAs:					
TP73-AS1	TNBC	release the miR-490-3p's post-translational repression on Twist1	miR-490-3p	promote	(Tao et al., 2018)
LINC00312	lung adenocarcinoma	YBX1 as the interacting partner to increase VE-cadherin, TGF-β, VEGF-A/-C levels *via* AKT	unknown	promote	(Peng et al., 2018)
MALAT1	non-small cell lung cancer	upregulated upon ERβ activation, prevent NEDD9 repression	miR-145-5p	promote	(Yu et al., 2019)
	gastric cancer	ERK/MMP and FAK/paxillin signaling	miR-376a		(Li, Wu, et al., 2017b)
n339260	HCC	linked to c-Myc/SOX2 overexpression; increase VE-cadherin levels	miR-31-3p, miR-30e-5p, miR-520c-5p, miR-519c-5p, miR-29b-1-5p	promote	(Zhao et al., 2018)
LINC00339	glioma	activate Twist1/MMP-2/MMP-14 signaling	miR-539-5p	promote	(Guo et al., 2018)
HOXA-AS2	glioma	downstream EGFR signaling, increase VE-cadherin and MMP-2/—9 levels	miR-373	promote	(Gao et al., 2018)
ZNRD1-AS1	glioma	regulate ELF1/EMI1 axis	miR-499a-5p	promote	(Wang, Song, et al., 2020a, Wang, Yang, et al., 2020b)
SNHG20	glioma	increase SNHG20 stability, promote FOXK1 degradation and increase MMP-1/—9 and VE-cadherin levels	unknown	promote	(Li et al., 2019)
HCG15	glioma	ZNF331 targeting	unknown	promote	(Jing et al., 2020)

Table 2
Summary of therapeutics targeting vasculogenic mimicry.

Molecules	Experimental model	References
HDAC inhibitors		
Vorinostat Trichostatin A Entinostat (MS275) MC1568	U87MG cells & GSCs	(Pastorino et al., 2019)
Entinostat (MS275)	Triple-negative breast cancer cells (MDA-MB-231, LM2-4,BT-549, MCF-7 cells)	(Maiti et al., 2019)
CSCinhibitors		
Salinomycin	CSCs	(Gupta et al., 2009)
Tyrosine kinase inhibitors		
Anti-VEGFR1-mAb (D16F7)	Melanoma & glioblastoma	(Graziani et al., 2016); (Atzori et al., 2017)
Sorafenib	HCC patients	(Mao et al., 2020)
MMP inhibitors		
Incyclinide derivative (COL-3)	Metastatic cancers	NCT00001683
Doxycycline	NCI-H446, A549 cells & HCC	(Ko et al., 2015); (Cao et al., 2013); (Meng et al., 2014)
TGF-βR1 antagonist		
Galunisertib	Glioma	(Zhang et al., 2016)
Molecules from plants:		
Brucine	MDA-MB-231 cells	(Xu et al., 2019)
Polyphyllin I	HCC	(Xiao et al., 2018)
Lupeol	B16F10 cells	(Bhattacharyya et al., 2019)